

1 The ubiquitin ligase HUWE1 enhances WNT signaling by antagonizing destruction complex-
2 mediated β -catenin degradation and through a mechanism independent of β -catenin stability

3

4 Short Title: HUWE1 enhances WNT signaling via two mechanisms

5

6 Joseph K. McKenna^{1¶}, Yalan Wu^{1¶}, Praveen Sonkusre¹, Raj Chari² and Andres M. Lebensohn^{1*}

7

8 ¹ Laboratory of Cellular and Molecular Biology, Center for Cancer Research, National Cancer
9 Institute, National Institutes of Health, Bethesda, Maryland, United States of America.

10 ² Genome Modification Core, Laboratory Animal Sciences Program, Frederick National Lab for
11 Cancer Research, Frederick, Maryland, United States of America.

12

13 * Corresponding author

14 E-mail: andres.lebensohn@nih.gov (AML)

15

16 ¶ These authors contributed equally to this work and are listed in the order in which they started
17 working on this project.

18

19 **Abstract:**

20

21 WNT/ β -catenin signaling is mediated by the transcriptional coactivator β -catenin (CTNNB1).
22 CTNNB1 abundance is regulated by phosphorylation and proteasomal degradation promoted by
23 a destruction complex composed of the scaffold proteins APC and AXIN1 or AXIN2, and the
24 kinases CSNK1A1 and GSK3A or GSK3B. Loss of CSNK1A1 increases CTNNB1 abundance,
25 resulting in hyperactive WNT signaling. Previously, we demonstrated that the HECT domain
26 ubiquitin ligase HUWE1 is necessary for hyperactive WNT signaling in HAP1 haploid human
27 cells lacking CSNK1A1. Here, we investigate the mechanism underlying this requirement. In the
28 absence of CSNK1A1, GSK3A/GSK3B still phosphorylated a fraction of CTNNB1, promoting
29 its degradation. HUWE1 loss enhanced GSK3A/GSK3B-dependent CTNNB1 phosphorylation,
30 further reducing CTNNB1 abundance. However, the reduction in CTNNB1 caused by HUWE1
31 loss was disproportionately smaller than the reduction in WNT target gene transcription. To test
32 if the reduction in WNT signaling resulted from reduced CTNNB1 abundance alone, we
33 engineered the endogenous *CTNNB1* locus in HAP1 cells to encode a CTNNB1 variant
34 insensitive to destruction complex-mediated phosphorylation and degradation. HUWE1 loss in
35 these cells reduced WNT signaling with no change in CTNNB1 abundance. Genetic interaction
36 and overexpression analyses revealed that the effects of HUWE1 on WNT signaling were not
37 only mediated by GSK3A/GSK3B, but also by APC and AXIN1. Regulation of WNT signaling
38 by HUWE1 required its ubiquitin ligase activity. These results suggest that in cells lacking
39 CSNK1A1, a destruction complex containing APC, AXIN1 and GSK3A/GSK3B downregulates
40 WNT signaling by phosphorylating and targeting CTNNB1 for degradation. HUWE1 enhances
41 WNT signaling by antagonizing this activity. Therefore, HUWE1 enhances WNT/CTNNB1

42 signaling through two mechanisms, one that regulates CTNNB1 abundance and another that is
43 independent of CTNNB1 stability. Coordinated regulation of CTNNB1 abundance and an
44 independent signaling step by HUWE1 would be an efficient way to control WNT signaling
45 output, enabling sensitive and robust activation of the pathway.

46

47 **Author Summary**

48

49 The WNT pathway is a conserved signaling system with diverse functions in embryonic
50 development and adult tissue homeostasis. Dysregulation of WNT signaling drives many types
51 of cancer. Over four decades of research have revealed a great deal about how the core
52 components of the WNT pathway regulate signaling, but much less is known about additional
53 regulatory layers superimposed on the core signaling module. In this study we present an
54 example of such regulation by the ubiquitin ligase HUWE1. Phosphorylation of the
55 transcriptional co-activator β -catenin by a protein complex called the destruction complex targets
56 β -catenin for degradation. This is considered the main regulated step in WNT signaling. We
57 demonstrate that HUWE1 enhances WNT signaling through two distinct mechanisms. First,
58 HUWE1 antagonizes the phosphorylation and degradation of β -catenin by the destruction
59 complex. Second, HUWE1 enhances WNT signaling through a mechanism independent from
60 control of β -catenin stability. The effects of HUWE1 on WNT signaling require its ubiquitin
61 ligase activity, suggesting there is a HUWE1 substrate awaiting discovery. Our work therefore
62 reveals a new role for HUWE1 controlling the main regulated step in WNT signaling – β -catenin
63 phosphorylation by the destruction complex – and most likely a downstream mechanism.

64

65 **Introduction:**

66

67 During embryonic development and tissue homeostasis, WNT/ β -catenin signaling orchestrates
68 cellular processes that control tissue patterning and morphogenesis, cell fate specification, and
69 stem cell self-renewal among many other functions [1, 2]. Mutations in WNT signaling pathway
70 components can drive tumorigenesis of many cancer types, most notably colorectal cancer [3, 4].
71 At the heart of the WNT/ β -catenin signaling pathway, the destruction complex (DC) controls the
72 abundance of the transcriptional coactivator β -catenin (CTNNB1) by regulating its degradation
73 through the ubiquitin/proteasome system. The DC is comprised of a set of core components,
74 including the scaffold proteins APC and AXIN1 or AXIN2, and the kinases casein kinase 1 α
75 (CSNK1A1) and glycogen synthase kinase 3 α (GSK3A) or β (GSK3B) [5]. In the absence of
76 signals initiated by secreted WNT ligands, CSNK1A1 phosphorylates CTNNB1 at serine (S) 45
77 [6, 7], priming it for further sequential phosphorylation of threonine (T) 41, S37 and S33 by
78 GSK3A and/or GSK3B [6, 8] (we refer to residues S33, S37, T41 and S45 as the CTNNB1
79 phosphodegron). When phosphorylated, residues S33 and S37 create a recognition site for the
80 ubiquitin ligase complex SCF ^{β TrCP} [9, 10], which ubiquitylates CTNNB1 and targets it for
81 proteasomal degradation [5]. Therefore, CTNNB1 abundance is kept low and WNT-dependent
82 transcriptional programs are repressed. Binding of WNT ligands to the cell surface receptors
83 frizzled (FZD) and LDL receptor related proteins 5 (LRP5) or 6 (LRP6) triggers the recruitment
84 of dishevelled (DVL) and at least some DC components to FZD and LRP5/6. Formation of this
85 receptor complex, or signalosome, downregulates the DC [11, 12] and results in accumulation of
86 non-phosphorylated CTNNB1. CTNNB1 enters the nucleus, where it forms a complex with

87 transcription factors of the TCF/LEF family and other coactivators to drive WNT target gene
88 transcription [13].

89 This description of WNT/CTNNB1 signaling omits additional regulatory mechanisms
90 superimposed on the core pathway that control the abundance, interactions, and subcellular
91 localization of many components of the pathway. Such additional regulatory mechanisms tune
92 WNT responses in diverse biological contexts, expand the functional repertoire of the pathway,
93 and may represent potential sites of therapeutic intervention in WNT-driven cancers. Classical
94 genetic approaches have been very successful at discovering new regulation in WNT signaling
95 [14]. In a previous study, we sought to uncover new regulatory mechanisms in WNT signaling
96 by performing forward genetic screens in HAP1-7TGP cells, a derivative of the haploid human
97 cell line HAP1 harboring a fluorescent reporter of WNT signaling [15]. HAP1 cells are
98 especially well suited for genetic screens due to the presence of a single allele of most genes in
99 their near-haploid genome, which can be disrupted by mutagenesis to generate true genetic null
100 cells [16]. We previously reported a comprehensive set of forward genetic screens designed to
101 identify positive, negative and attenuating regulators of WNT/CTNNB1 signaling, as well as
102 regulators of R-spondin (RSPO) signaling and suppressors of hyperactive WNT signaling
103 induced by loss of distinct DC components, including APC and CSNK1A1 [15]. These screens
104 recovered hits implicated at several levels of the pathway, including WNT and RSPO reception
105 at the plasma membrane, cytosolic signal transduction, and transcriptional regulation.
106 Comparative analyses of the screens enabled us to infer genetic interactions based on distinct
107 patterns of hits identified by the different screens. The screens for suppressors of hyperactive
108 signaling induced by loss of APC or CSNK1A1 suggested potential candidates for targeting
109 oncogenic WNT signaling.

110 An unexpected outcome of the *APC* and *CSNK1A1* suppressor screens was that we
111 observed only a partial overlap between significant hits in the two screens [15]. The phenotypic
112 selection parameters used in both screens were the same and the cell lines used for the two
113 screens were isogenic except for the mutations in *APC* or *CSNK1A1* we introduced by
114 CRISPR/Cas9-mediated genome editing. Therefore, we expected that the hits identified in the
115 two suppressor screens would be the same. After all, if APC and CSNK1A1 regulate
116 WNT/CTNNB1 signaling through a single common function in the DC phosphorylating
117 CTNNB1, we assumed that hyperactivating the pathway by knocking out one or the other would
118 be functionally equivalent, and the complement of downstream regulators would be shared.
119 While there were indeed many common hits with high significance scores in both suppressor
120 screens, including established downstream regulators of WNT/CTNNB1 signaling such as
121 *CTNNB1* and *CREBBP*, there were also many hits unique to the *APC* suppressor or the
122 *CSNK1A1* suppressor screen [15]. These results suggested that the hyperactive signaling state
123 resulting from loss of these two DC components was not equivalent. We hypothesized that the
124 difference in potential downstream regulators in the two genetic backgrounds in which the
125 screens were conducted – *APC* knock-out (KO) or *CSNK1A1* KO – could reflect additional roles
126 of APC or CSNK1A1 in WNT/CTNNB1 signaling beyond their shared function regulating
127 CTNNB1 stability.

128 *HUWE1*, the gene encoding the eponymous ubiquitin ligase, was the most striking
129 example of a hit that was highly significant in the *CSNK1A1* suppressor but not the *APC*
130 suppressor screen [15]. HUWE1 is a very large, 482 kilodalton (kDa) HECT domain ubiquitin
131 ligase that has been implicated in many cellular processes, including transcriptional regulation,
132 DNA replication and repair, cell cycle arrest, cell adhesion, cell migration, cell proliferation and

133 differentiation, proteotoxic stress, ribosome biogenesis, mitochondrial maintenance, autophagy,
134 apoptosis and WNT signaling [17-20]. *HUWE1* was the third most significant hit in the
135 *CSNK1A1* suppressor screen, surpassed only by *CTNNB1* and *CREBBP*, which encode two of
136 the main components of the TCF/LEF transcription complex and are therefore central players in
137 the WNT pathway [15]. However, *HUWE1* was not a significant hit in the *APC* suppressor
138 screen (rank number 8040 out of 11022 genes with mapped gene-trap integrations), and it was
139 not among the most significant hits in any of the screens performed in wild-type (WT) HAP1-
140 7TGP cells, designed to identify positive regulators of WNT3A- and RSPO1-induced signaling.
141 These results suggested that *HUWE1* might be involved in a regulatory mechanism that is most
142 evident in the *CSNK1A1*^{KO} genetic background (for brevity, HAP1-7TGP cell lines in which
143 genes were disrupted will be referred to by the name of the protein encoded by the targeted gene
144 or genes followed by a “KO” superscript). In follow-up studies, we had confirmed that *HUWE1*
145 loss reduced WNT target gene transcription – and to a smaller extent *CTNNB1* abundance – in
146 *CSNK1A1*^{KO} but not in *APC*^{KO} cells [15]. We had also shown that microinjection of *HUWE1*
147 mRNA into *Xenopus laevis* embryos promoted body axis duplication, a hallmark of ectopic
148 WNT signaling [15]. These experiments established a few biological contexts in which *HUWE1*
149 acts as a positive regulator of WNT/*CTNNB1* signaling, but the underlying mechanism remained
150 unclear and the reason why *HUWE1* loss selectively reduced WNT/*CTNNB1* signaling in
151 *CSNK1A1*^{KO} cells remained unknown.

152 Here we extend our genetic analyses to show that *HUWE1* enhances WNT/*CTNNB1*
153 signaling through two different mechanisms. First, *HUWE1* reduces phosphorylation of the
154 *CTNNB1* phosphodegron by antagonizing the activity of a DC composed of GSK3A/GSK3B,

155 APC and AXIN1, therefore increasing CTNNB1 abundance. Second, HUWE1 enhances WNT
156 signaling through a mechanism that is independent from the control of CTNNB1 stability.
157

158 **Results:**

159

160 **HUWE1 enhances WNT signaling in CSNK1A1^{KO} cells by antagonizing GSK3A/GSK3B-**
161 **dependent phosphorylation of the CTNNB1 phosphodegron and increasing CTNNB1**
162 **abundance**

163

164 We previously reported that HUWE1 loss in CSNK1A1^{KO} cells caused a substantial, 80-90%
165 reduction in WNT reporter activity and endogenous WNT target gene expression that was
166 accompanied by a smaller, 20-32% reduction in soluble CTNNB1 abundance [15]. Soluble
167 CTNNB1 is a proxy for the signaling CTNNB1 pool because it excludes the more stable, plasma
168 membrane-associated junctional CTNNB1 pool. We readily reproduced these results in the
169 current study: HUWE1 loss in CSNK1A1^{KO} cells reduced WNT reporter activity by 89% and
170 soluble CTNNB1 abundance by 36% (Figs 1A and 1B, and S1A Fig). These results raised the
171 possibility that in CSNK1A1^{KO} cells, HUWE1 loss reduces WNT signaling solely by reducing
172 CTNNB1 abundance, but that a non-linear relationship between changes in CTNNB1 abundance
173 and transcriptional activity results in a disproportionately greater reduction in WNT target gene
174 expression than CTNNB1 abundance. Alternatively, HUWE1 could regulate both CTNNB1
175 abundance and another process, which when disrupted together following HUWE1 loss result in
176 a greater reduction in WNT target gene expression than in CTNNB1 abundance. To distinguish
177 between these possibilities, we thought it was important to first determine the mechanism
178 underlying the reduction in CTNNB1 abundance caused by HUWE1 loss.

179 The main mechanism regulating CTNNB1 abundance is phosphorylation of the CTNNB1
180 phosphodegron by the DC [5]. In CSNK1A1^{KO} cells we did not expect the phosphodegron to be

181 phosphorylated by GSK3A/GSK3B at residues S33, S37 and T41 because phosphorylation of
182 these residues generally requires the priming phosphorylation of residue S45 by CSNK1A1 [6,
183 7]. Nevertheless, we tested whether the reduction in CTNNB1 abundance caused by HUWE1
184 loss in CSNK1A1^{KO} cells was due to changes in phosphorylation of the CTNNB1
185 phosphodegron. CTNNB1 phosphorylated at S33, S37 and T41 can be measured directly by
186 Western blot, but due to the rapid proteasomal degradation of this species, treatment with
187 proteasome inhibitors is usually required to make such measurements [7]. Since any effects of
188 HUWE1 on WNT signaling could conceivably also depend on proteasomal degradation of a
189 HUWE1 substrate, which would be disrupted by proteasome inhibitors, we opted for a different
190 way to evaluate phosphorylation of the CTNNB1 phosphodegron. We instead quantified
191 CTNNB1 that is *not* phosphorylated at residues S33, S37 and T41 (we refer to this species as
192 non-phospho-CTNNB1, but it is also known as active CTNNB1 [21]) from whole cell extracts
193 (WCE) (Figs 1C and S1B Fig). As a control, we also measured total CTNNB1 from WCE (S1B
194 and S1C Figs). Non-phospho-CTNNB1 abundance in the various conditions tested was different
195 from and exhibited larger changes than total CTNNB1 abundance (Fig 1C, and S1B and S1C
196 Figs). This indicated that non-phospho-CTNNB1 only represents a fraction of the total CTNNB1
197 in WCE and is likely to accurately reflect changes in phosphorylation of the CTNNB1
198 phosphodegron.

199 HUWE1 loss in CSNK1A1^{KO} cells reduced non-phospho-CTNNB1 abundance by 37%, a
200 reduction that correlated closely with the 36% reduction in soluble CTNNB1 abundance caused
201 by HUWE1 loss in the same cell line (Figs 1B and 1C, and S1A and S1B Figs). This correlation
202 suggested that the reduction in CTNNB1 abundance caused by HUWE1 loss was due to
203 increased CTNNB1 phosphorylation at S33, S37 and T41, presumably mediated by

204 GSK3A/GSK3B. If this were the case, inhibiting GSK3A/GSK3B should reverse the reduction
205 in both soluble and non-phospho-CTNNB1 abundance caused by HUWE1 loss. Treatment of
206 CSNK1A1^{KO}; HUWE1^{KO} cells with the GSK3A/GSK3B inhibitor CHIR-99021 indeed increased
207 the abundance of soluble CTNNB1 by 2.4-fold and the abundance of non-phospho-CTNNB1 by
208 3.2-fold (Figs 1B and 1C, and S1A and S1B Figs), entirely reversing the reductions caused by
209 HUWE1 loss. Furthermore, GSK3A/GSK3B inhibition in CSNK1A1^{KO}; HUWE1^{KO} cells
210 increased WNT reporter activity by 10.9-fold, restoring signaling to a comparable level to that in
211 DMSO vehicle-treated CSNK1A1^{KO} cells (Fig 1A). These results indicate that even in the
212 absence of CSNK1A1, phosphorylation of residues S33, S37 and T41 by GSK3A/GSK3B can
213 regulate CTNNB1 abundance, and that HUWE1 loss reduces CTNNB1 abundance and WNT
214 signaling by promoting the phosphorylation of these residues.

215 Since HUWE1 loss in CSNK1A1^{KO} cells increased GSK3A/GSK3B-dependent
216 phosphorylation of the CTNNB1 phosphodegron, we wondered whether in CSNK1A1^{KO} cells
217 containing HUWE1, residues S33, S37 and T41 in the phosphodegron might be partially
218 phosphorylated by GSK3A/GSK3B despite the absence of CSNK1A1. CSNK1A1^{KO} cells had a
219 relatively high abundance of soluble and non-phospho-CTNNB1, as well as high WNT reporter
220 activity, compared to basal levels in unstimulated WT HAP1-7TGP cells (Figs 1A-C, and S1A
221 and S1B Figs). However, GSK3A/GSK3B inhibition with CHIR-99021 in CSNK1A1^{KO} cells
222 increased the abundance of soluble CTNNB1 by 1.6-fold and the abundance of non-phospho-
223 CTNNB1 by 1.8-fold (Figs 1B and 1C, and S1A and S1B Figs). WNT reporter activity also
224 increased 1.7-fold following treatment of CSNK1A1^{KO} cells with CHIR-99021 (Fig 1A).
225 Therefore, in the absence of CSNK1A1, residual GSK3A/GSK3B-dependent phosphorylation of

226 the CTNNB1 phosphodegron can still take place. This is presumably followed by ubiquitylation
227 and proteasomal degradation of phosphorylated CTNNB1.

228 In summary, in CSNK1A1^{KO} cells, CTNNB1 is still phosphorylated by GSK3A/GSK3B at
229 residues S33, S37 and S41 in the CTNNB1 phosphodegron, and the reduction in soluble
230 CTNNB1 abundance caused by HUWE1 loss is due to increased GSK3A/GSK3B-dependent
231 phosphorylation of these residues. We conclude that when present, HUWE1 antagonizes the
232 GSK3A/GSK3B-dependent phosphorylation and ensuing degradation of CTNNB1, thereby
233 increasing CTNNB1 abundance and promoting WNT signaling.

234 Our results raise two important questions. First, is control of CTNNB1 phosphorylation and
235 abundance the only mechanism whereby HUWE1 enhances WNT signaling, or is there another
236 mechanism distinct from the control of CTNNB1 stability? Second, is the GSK3A/GSK3B-
237 dependent regulation of CTNNB1 abundance by HUWE1, and potentially any other mechanisms
238 by which HUWE1 enhances WNT signaling, also mediated by other components of the DC in
239 addition to GSK3A/GSK3B? We addressed both these questions.

240

241 **HUWE1 enhances WNT signaling through a mechanism independent of CTNNB1 stability**

242

243 We next sought to determine if HUWE1 could promote WNT signaling through additional
244 mechanisms distinct from control of CTNNB1 phosphorylation and abundance. Mutations in the
245 CTNNB1 phosphodegron that prevent phosphorylation by CSNK1A1 and GSK3A/GSK3B
246 render CTNNB1 insensitive to degradation by the DC [6, 7, 22]. We reasoned that introducing
247 such mutations into the single *CTNNB1* allele of HAP1-7TGP cells would enable us to decouple

248 control of CTNNB1 abundance from any other mechanism by which HUWE1 enhances WNT
249 signaling.

250 We used CRISPR/Cas9-induced homology directed repair (HDR) to edit the codons
251 encoding CSNK1A1 and GSK3A/GSK3B phosphorylation sites in the phosphodegron of the
252 single endogenous *CTNNB1* locus in HAP1-7TGP cells. We introduced mutations encoding
253 alanine (A) substitutions in the codon encoding S45, which is phosphorylated by CSNK1A1, and
254 in the codons encoding T41 and S37, which are sequentially phosphorylated by GSK3A/GSK3B
255 (S1 File and S2A Fig). We were unable to mutate S33, the third GSK3A/GSK3B target site.
256 However, recognition of CTNNB1 by SCF^{βTrCP} requires phosphorylation of both S33 and S37 [9,
257 10], and therefore the mutations we introduced still prevented DC-dependent CTNNB1
258 degradation, as we demonstrate below. We called the resulting HAP1-7TGP derivative cell line
259 CTNNB1^{ST-A}. The mutations in the *CTNNB1* locus of CTNNB1^{ST-A} cells indeed increased
260 soluble CTNNB1 abundance 42-fold compared to unstimulated WT HAP1-7TGP cells (Fig 2A
261 and S2B Fig), and promoted constitutive WNT signaling as judged by WNT reporter activity and
262 endogenous WNT target gene (*AXIN2* [23], *RNF43* [23], *NKD1* [24], *TNFRSF19* [25])
263 expression (Figs 2B-F). Furthermore, CTNNB1 abundance, WNT reporter activity and WNT
264 target gene expression in CTNNB1^{ST-A} cells were substantially higher than in WT HAP1-7TGP
265 cells treated with a near-saturating dose of WNT3A conditioned media (CM) (Figs 2A-F, and
266 S2B Fig). Stimulation of CTNNB1^{ST-A} cells with WNT3A CM did not significantly increase
267 total CTNNB1 abundance or WNT target gene expression (S2C-E Figs). These results confirmed
268 that the mutations we introduced into CTNNB1^{ST-A} cells rendered CTNNB1 insensitive to
269 degradation by the DC, and therefore abolished the control of CTNNB1 stability by WNT
270 ligands.

271 We then knocked out *HUWE1* in CTNNB1^{ST-A} cells (S1 File and S2B Fig) and measured the
272 effect on CTNNB1 abundance and WNT signaling. HUWE1 loss in multiple independent clonal
273 cell lines (CTNNB1^{ST-A}; HUWE1^{KO}) did not affect soluble CTNNB1 abundance (Fig 2A and
274 S2B Fig), but significantly reduced WNT reporter activity (Fig 2B and S2F Fig) and the
275 expression of some WNT target genes (Figs 2C-F). These results demonstrate that HUWE1 loss
276 reduces WNT signaling in part through a mechanism independent from the control of CTNNB1
277 stability. We also note that the 49% reduction in WNT reporter activity, 45% reduction in *AXIN2*
278 expression and 31% reduction in *RNF43* expression caused by HUWE1 loss in CTNNB1^{ST-A}
279 cells (Figs 2B-D and S2F Fig) were smaller than the 89% reduction in WNT reporter activity,
280 67% reduction in *AXIN2* expression and 73% reduction in *RNF43* expression caused by HUWE1
281 loss in CSNK1A1^{KO} cells (Figs 1A and 3C-D). This difference could be because in CSNK1A1^{KO}
282 cells, HUWE1 loss caused a 31-36% reduction in soluble CTNNB1 abundance (Figs 1B and 3A-
283 B, and S1A Fig) in addition to the reduction in signaling caused by the second regulatory
284 mechanism that is independent from changes in CTNNB1 abundance, whereas no corresponding
285 reduction in CTNNB1 abundance was observed following HUWE1 loss in CTNNB1^{ST-A} cells
286 (Fig 2A and S2B Fig).

287 In summary, we distinguished two mechanisms whereby HUWE1 loss reduces WNT
288 signaling. In CSNK1A1^{KO} cells containing WT CTNNB1, HUWE1 loss caused a moderate
289 reduction in CTNNB1 abundance and a comparable increase in GSK3A/GSK3B-dependent
290 phosphorylation of the CTNNB1 phosphodegron, as well as a much larger GSK3A/GSK3B-
291 dependent reduction in WNT reporter activity (Fig 1). In CTNNB1^{ST-A} cells containing WT
292 CSNK1A1 but a mutated CTNNB1 phosphodegron, HUWE1 loss did not alter CTNNB1
293 abundance but still caused a significant reduction in WNT reporter activity and WNT target gene

294 expression (Fig 2). We conclude that HUWE1 enhances WNT signaling through two distinct
295 mechanisms, one that increases CTNNB1 abundance and one that is independent of CTNNB1
296 stability.

297

298 **HUWE1 enhances WNT signaling through mechanisms mediated by APC**

299

300 Having defined two mechanisms whereby HUWE1 regulates WNT signaling, a
301 GSK3A/GSK3B-dependent mechanism that controls CTNNB1 phosphorylation and abundance,
302 and another mechanism that is independent from the control of CTNNB1 stability, we wondered
303 whether these mechanisms were also mediated by other DC components. HUWE1 was one of
304 the most significant hits in a *CSNK1A1* suppressor screen but was not a significant hit in an *APC*
305 suppressor screen [15]. Consistent with the results of these screens, HUWE1 loss substantially
306 reduced WNT reporter activity in *CSNK1A1*^{KO} cells but did not affect WNT reporter activity in
307 *APC*^{KO} cells [15]. Based on these results, we hypothesized that APC may be required to mediate
308 the effects of HUWE1 on WNT signaling. If APC is required for the reduction in WNT signaling
309 caused by HUWE1 loss in *CSNK1A1*^{KO} cells, then eliminating APC function in *CSNK1A1*^{KO};
310 *HUWE1*^{KO} cells, like inhibiting GSK3A/GSK3B activity (Fig 1), should reverse said reduction.
311 To the best of our knowledge, there are no pharmacological inhibitors that we could use to
312 acutely inhibit APC. We were also unable to knock out *APC* in *CSNK1A1*^{KO}; *HUWE1*^{KO} cells,
313 as we found that knocking out additional genes by CRISPR/Cas9-mediated genome editing in
314 this cell line yielded very few viable clones. Instead, we first made cell lines lacking both APC
315 and *CSNK1A1*, and then tested the effects of HUWE1 loss in these cells, comparing them to
316 cells lacking *CSNK1A1* alone.

317 *CSNK1A1* single KO clonal HAP1-7TGP cell lines were generated and characterized
318 previously [15] (*CSNK1A1*^{KO-1} and *CSNK1A1*^{KO-2}; we note that *CSNK1A1*^{KO-2} is a loss-of-
319 function allele containing a two amino acid deletion). We generated two new *APC* single KO
320 clonal HAP1-7TGP cell lines (*APC*^{KO-1} and *APC*^{KO-2}) as well as two new *APC* and *CSNK1A1*
321 double KO clonal HAP1-7TGP cell lines (*APC*^{KO-1}; *CSNK1A1*^{KO-1} and *APC*^{KO-1}; *CSNK1A1*^{KO-2}
322 ²) using CRISPR/Cas9-mediated genome editing. We validated these cell lines by sequencing
323 each targeted locus (S1 File), and by Western blot analysis (Fig 3A). *CSNK1A1*^{KO}, *APC*^{KO} and
324 *APC*^{KO}; *CSNK1A1*^{KO} cells all exhibited elevated soluble CTNNB1 abundance several-fold
325 higher than unstimulated WT HAP1-7TGP cells (Figs 3A and 3B). All these clonal cell lines
326 exhibited constitutive expression of WNT target genes several-fold higher than the level of gene
327 expression in unstimulated WT HAP1-7TGP cells and in WT HAP1-7TGP cells stimulated with
328 a near-saturating dose of WNT3A CM (Figs 3C-F). Consistent with our results demonstrating
329 that in *CSNK1A1*^{KO} cells residual phosphorylation of the CTNNB1 phosphodegron by
330 GSK3A/GSK3B results in some CTNNB1 degradation (Fig 1), both soluble CTNNB1
331 abundance and WNT target gene expression were higher in *APC*^{KO} and *APC*^{KO}; *CSNK1A1*^{KO}
332 cells than in *CSNK1A1*^{KO} cells (Figs 3A-F). These results support the notion that in HAP1 cells
333 *CSNK1A1* is partially dispensable for CTNNB1 phosphorylation by GSK3A/GSK3B.

334 We then knocked out *HUWE1* in *CSNK1A1*^{KO}, *APC*^{KO} and *APC*^{KO}; *CSNK1A1*^{KO} cells to
335 generate three *CSNK1A1*^{KO}; *HUWE1*^{KO}, three *APC*^{KO}; *HUWE1*^{KO} and three *APC*^{KO};
336 *CSNK1A1*^{KO}; *HUWE1*^{KO} clonal cell lines, which we validated by sequencing the targeted
337 *HUWE1* locus (S1 File) and by Western blot analysis (Fig 3A). *HUWE1* loss in *CSNK1A1*^{KO}
338 cells substantially reduced the expression of all WNT target genes tested (Figs 3C-F) and, to a
339 lesser extent, soluble CTNNB1 abundance (Figs 3A and 3B). In contrast, *HUWE1* loss in *APC*^{KO}

340 cells resulted in a variable but not statistically significant reduction in WNT target gene
341 expression (Figs 3C-F) and did not reduce soluble CTNNB1 abundance (Figs 3A and 3B),
342 consistent with our previous finding that HUWE1 loss in APC^{KO} cells had no effect on WNT
343 reporter activity [15]. Finally, HUWE1 loss in APC^{KO}; CSNK1A1^{KO} cells yielded equivalent
344 results to those in APC^{KO} cells, showing no significant reduction in WNT target gene expression
345 (Figs 3C-F) or soluble CTNNB1 abundance (Figs 3A and 3B). These results indicate that, like
346 GSK3A/GSK3B inhibition, APC loss precludes the reduction in WNT target gene expression
347 and CTNNB1 abundance caused by HUWE1 loss in CSNK1A1^{KO} cells. We conclude that APC
348 mediates the effects of HUWE1 on WNT signaling.

349

350 **HUWE1 enhances WNT signaling through mechanisms mediated by a subset of DC**
351 **components including APC, AXIN1 and GSK3A or GSK3B**

352

353 We extended the same logic as for APC (Fig 3) to test the role of every core component of the
354 DC in mediating the functions of HUWE1 in WNT signaling. We first knocked out components
355 of the DC individually or in certain combinations (Table 1) so we could then test the effects of
356 HUWE1 loss on WNT signaling in each of these mutant genetic backgrounds. While we had
357 already established the role of GSK3A/GSK3B and APC in mediating HUWE1 functions (Figs 1
358 and 3), we included them in our analysis to confirm those results and, in the case of GSK3A and
359 GSK3B, test their roles individually. We used CRISPR/Cas9-mediated genome editing to
360 generate HAP1-7TGP clonal cell lines lacking the desired DC components (Table 1). We
361 confirmed that each targeted genomic locus had been successfully mutated (S1 File) and that the
362 encoded protein had been eliminated (S4A Fig).

363

364 **Table 1. HUWE1 enhances WNT signaling through mechanisms mediated by a subset of**

365 **DC components including APC, AXIN1 and GSK3A or GSK3B.**

366

Genotype	Aggregate WNT target gene expression, average of HUWE1 sgRNA1 and sgRNA2 (% of SCR sgRNA control)	Significance of change in aggregate WNT target gene expression for HUWE1 sgRNA 1/2 relative to SCR sgRNA control
WT - WNT3A	101	n.s./n.s.
WT + WNT3A	70	*/*
CSNK1A1 ^{KO}	47.5	**/**
APC ^{KO}	86.5	n.s./n.s.
APC ^{KO} ; CSNK1A1 ^{KO}	86	n.s./n.s.
AXIN1 ^{KO} ; AXIN2 ^{KO}	91.5	n.s./n.s.
CSNK1A1 ^{KO} ; AXIN1 ^{KO} ; AXIN2 ^{KO}	103	n.s./n.s.
CSNK1A1 ^{KO} ; AXIN1 ^{KO}	95	n.s./n.s.
CSNK1A1 ^{KO} ; AXIN2 ^{KO}	45.5	**/**
GSK3A ^{KO} ; GSK3B ^{KO}	88	n.s./n.s.
CSNK1A1 ^{KO} ; GSK3A ^{KO} ; GSK3B ^{KO}	141.5	*/n.s.
CSNK1A1 ^{KO} ; GSK3A ^{KO}	53	**/**
CSNK1A1 ^{KO} ; GSK3B ^{KO}	40	**/**

367

368 Summary of effects of CRISPRi-mediated HUWE1 KD on aggregate WNT target gene

369 expression (Fig 4A). For the genotypes treatments indicated in green, both HUWE1 sgRNAs

370 used resulted in a significant reduction in aggregate WNT target gene expression relative to the

371 SCR sgRNA control.

372

373 To test the effects of HUWE1 loss in each of these mutant cell lines, we adopted a different

374 experimental strategy. We had previously quantified the effect of HUWE1 loss on WNT

375 signaling through an experimental scheme that we refer to as clonal analysis. In this scheme, we

376 used CRISPR/Cas9-mediated genome editing to target *HUWE1*. We isolated multiple

377 independent clonal cell lines in which *HUWE1* had been knocked out, and multiple clonal cell

378 lines that remained WT at the targeted locus to use as controls. We then compared several KO

379 and WT clones for WNT reporter activity or other parameters of interest (Figs 2 and 3, and S2F
380 Fig). While clonal analysis enables comparisons in true genetic null conditions, it is subject to
381 substantial inter-clonal variability, requiring the laborious isolation of many independent clones
382 to achieve statistical significance. Isolation of multiple clones harboring *HUWE1* mutations in
383 each of the 12 different genetic backgrounds (Table 1) in which we wanted to test the effect of
384 *HUWE1* loss was unfeasible. Therefore, we implemented a CRISPR interference (CRISPRi)-
385 mediated knock-down (KD) strategy [26] that enabled us to measure the outcome of knocking
386 down *HUWE1* in polyclonal cell populations rather than in multiple individual clonal cell lines.
387 We used a lentivirus to deliver the CRISPRi machinery together with sgRNAs targeting *HUWE1*
388 in the various cell lines we had generated lacking DC components (Table 1 and S4A Fig). Based
389 on Western blot measurements (S5A and S5B Figs), lentiviral delivery of either of two different
390 sgRNAs targeting *HUWE1* (*HUWE1* sgRNA1 or sgRNA2) followed by antibiotic selection of
391 transduced cells resulted in a consistent 59-95% KD of *HUWE1* compared to a control,
392 scrambled (SCR) sgRNA. We refer to polyclonal cell populations in which we knocked down
393 *HUWE1* using CRISPRi as *HUWE1*^{KD}, in contrast to *HUWE1*^{KO} clonal cell lines in which we
394 knocked out *HUWE1* using CRISPR/Cas9-mediated genome editing.

395 To validate the CRISPRi KD strategy, we tested whether knocking down *HUWE1* in
396 *CSNK1A1*^{KO}, *APC*^{KO}, and *APC*^{KO}; *CSNK1A1*^{KO} cell populations produced equivalent results to
397 those we had observed when we knocked out *HUWE1* and conducted clonal analysis in these
398 same cell lines (Fig 3). Consistent with our clonal analysis, *HUWE1* KD in *CSNK1A1*^{KO} cells
399 significantly reduced the expression of four WNT target genes compared to *CSNK1A1*^{KO} cells
400 transduced with SCR sgRNA (Figs 4A-E and Table 1). However, this reduction was smaller than
401 that caused by complete *HUWE1* loss in *CSNK1A1*^{KO}; *HUWE1*^{KO} cells (Figs 3C-F),

402 presumably owing to some residual HUWE1 protein present in CSNK1A1^{KO}; HUWE1^{KD} cells
403 (S5A and S5B Figs). Also consistent with our clonal analysis, HUWE1 KD in APC^{KO} and in
404 APC^{KO}; CSNK1A1^{KO} cells did not cause a statistically significant reduction in WNT target gene
405 expression (Figs 4A-E and Table 1). These results validate CRISPRi-mediated HUWE1 KD in
406 polyclonal cell populations as a reliable alternative to the more laborious clonal analysis of
407 multiple individual HUWE1^{KO} clonal cell lines. We also knocked down HUWE1 in WT HAP1-
408 7TGP cells (S5A and S5B Figs), in which we had previously reported that HUWE1 KO did not
409 cause a significant reduction in WNT reporter activity or *AXIN2* expression induced by a near-
410 saturating dose of WNT3A [15]. In agreement with those results, HUWE1 KD did not reduce
411 WNT3A-induced expression of *AXIN2* (Fig 4B). However, HUWE1 KD in WT HAP1-7TGP
412 cells did reduce the expression of other WNT target genes, including *RNF43*, *NKDI* and
413 *TNFRSF19*, but to a smaller extent than in CSNK1A1^{KO} cells (Figs 4A-E and Table 1). Together
414 with our analysis in CTNNB1^{ST-A} cells (Fig 2), these results demonstrate that the contribution of
415 HUWE1 to WNT signaling is not limited to cells lacking CSNK1A1.

416 We then asked whether other DC components mediate the function of HUWE1. As we had
417 done for APC, we tested whether knocking out AXIN1 and AXIN2 eliminated the reduction in
418 WNT signaling caused by HUWE1 loss. In WT HAP1-7TGP cells, AXIN1 and AXIN2 are
419 functionally redundant in their capacity to suppress WNT signaling, presumably by regulating
420 CTNNB1 abundance as scaffolds in the DC: eliminating either AXIN1 or AXIN2 has no effect
421 on WNT reporter activity, whereas eliminating both promotes constitutive pathway activation
422 [15]. We initially assumed that a possible role of AXIN1 and AXIN2 in mediating the effects of
423 HUWE1 may also be redundant, so we knocked out both paralogs in HAP1-7TGP cells (S1 File
424 and S4A Fig) and tested their contribution following HUWE1 KD (S5A and S5B Figs). HUWE1

425 KD in AXIN1^{KO}; AXIN2^{KO} cells did not reduce WNT target gene expression (Figs 4A-E and
426 Table 1), suggesting that AXIN1, AXIN2 or both mediate the effects of HUWE1 on WNT
427 signaling, similarly to what we had observed for APC (Fig 3). As we had done for
428 GSK3A/GSK3B (Fig 1) and APC (Fig 3), we also tested whether the combined loss of AXIN1
429 and AXIN2 eliminated the reduction in WNT signaling caused by HUWE1 KD in CSNK1A1^{KO}
430 cells. Indeed, knocking down HUWE1 in CSNK1A1^{KO}; AXIN1^{KO}; AXIN2^{KO} cells did not
431 reduce WNT target gene expression as it did in CSNK1A1^{KO} cells (Figs 4A-E and Table 1).
432 These results confirmed that AXIN1, AXIN2 or both mediate the effects of HUWE1 on WNT
433 signaling in CSNK1A1^{KO} cells. While AXIN1 and AXIN2 are redundant in their capacity to
434 suppress WNT signaling in WT HAP1-7TGP cells [15], it was conceivable that they may not be
435 redundant in mediating the function of HUWE1 in CSNK1A1^{KO} cells. To test for individual
436 contributions of AXIN1 or AXIN2, we knocked each of them out individually in CSNK1A1^{KO}
437 cells (S1 File and S4A Fig) and then knocked down HUWE1 (S5A and S5B Figs). AXIN1 loss
438 in CSNK1A1^{KO} cells eliminated the reduction in WNT signaling caused by HUWE1 KD, but
439 AXIN2 loss did not (Figs 4A-E and Table 1). These results suggest that, in contrast to its
440 redundant function with AXIN2 in suppressing WNT signaling in WT HAP1-7TGP cells [15],
441 AXIN1 plays a unique role in mediating HUWE1-dependent effects on WNT signaling that is
442 not redundant with AXIN2.

443 Given these results, we wondered whether GSK3A and GSK3B are redundant in mediating
444 the functions of HUWE1 in WNT signaling. To answer this question, we did an equivalent series
445 of experiments as the one we did to determine the individual roles of AXIN1 and AXIN2 in
446 mediating HUWE1 function. Like AXIN1 and AXIN2, GSK3A and GSK3B are functionally
447 redundant in their capacity to suppress WNT signaling in WT HAP1-7TGP cells: eliminating

448 either GSK3A or GSK3B has no effect on WNT reporter activity, whereas eliminating both
449 promotes constitutive pathway activation (S1 File, and S4B and S4C Figs). HUWE1 KD in
450 GSK3A^{KO}; GSK3B^{KO} cells (S5A and S5B Figs) did not reduce WNT target gene expression
451 (Figs 4A-E and Table 1), suggesting that GSK3A, GSK3B or both mediate the effects of
452 HUWE1 on WNT signaling. Next, we tested whether the combined loss of GSK3A and GSK3B
453 eliminated the reduction in WNT signaling caused by HUWE1 KD in CSNK1A1^{KO} cells.
454 Knocking down HUWE1 in CSNK1A1^{KO}; GSK3A^{KO}; GSK3B^{KO} cells (S5A and S5B Figs) did
455 not reduce – and in fact increased – WNT target gene expression (Figs 4A-E and Table 1). These
456 results confirmed that GSK3A, GSK3B or both mediate the effects of HUWE1 on WNT
457 signaling in CSNK1A1^{KO} cells. However, unlike their combined loss, loss of GSK3A or GSK3B
458 individually in CSNK1A1^{KO} cells did not eliminate the reduction in WNT signaling caused by
459 HUWE1 KD (Fig 4A-E and Table 1). We conclude that the role of GSK3A and GSK3B in
460 mediating HUWE1-dependent effects on WNT signaling is redundant, similarly to their role
461 suppressing WNT signaling in WT HAP1-7TGP cells (S4C Fig). Therefore, only the combined
462 loss of GSK3A and GSK3B eliminates the reduction in WNT signaling caused by HUWE1 KD
463 in CSNK1A1^{KO} cells (Fig 4A-E and Table 1).

464 We considered the possibility that the distinct outcomes of knocking down HUWE1 in the
465 various genetic backgrounds we tested (Table 1) could be due to differences in the steady state
466 abundance of HUWE1 caused by loss of some DC complex components but not others, rather
467 than due to other effects of distinct DC components in mediating HUWE1 function. Standard
468 Western blot analysis did not reveal obvious differences in steady state HUWE1 abundance
469 among the various genetic backgrounds in which we knocked down HUWE1 (S4A Fig). We
470 corroborated this result by quantitative dot blot analysis (see Materials and methods) and did not

471 detect significant differences in HUWE1 abundance among the different genetic backgrounds
472 (S4D Fig).

473 In conclusion, a subset of DC components, including APC, AXIN1 and GSK3A or GSK3B,
474 but not CSNK1A1 or AXIN2, mediates the function of HUWE1 in WNT signaling. Since
475 HUWE1 enhances WNT signaling by increasing CTNNB1 abundance (Fig 1) and through
476 another mechanism independent from the control of CTNNB1 stability (Fig 2), a DC composed
477 of APC, AXIN1 and GSK3A/GSK3B must mediate the effects of HUWE1 on one or both
478 mechanisms.

479

480 **HUWE1 enhances WNT signaling by antagonizing the DC**

481

482 The results presented so far are consistent with the following hypothesis: 1. In CSNK1A1^{KO}
483 cells, APC, AXIN1 and GSK3A/GSK3B are part of a DC that can partially suppress WNT
484 signaling by phosphorylating the CTNNB1 phosphodegron and targeting CTNNB1 for
485 proteasomal degradation; 2. HUWE1 enhances WNT signaling by antagonizing CTNNB1
486 phosphorylation and degradation mediated by this DC, and through another mechanism
487 independent of CTNNB1 stability. Whether the second mechanism is also mediated by the DC
488 remains unclear. Since all the data presented above were from loss-of-function genetic
489 experiments, we tested this hypothesis further through overexpression experiments. Based on
490 this hypothesis, we predicted that overexpressing the DC scaffold AXIN1 in CSNK1A1^{KO} cells
491 should increase DC activity and therefore have similar effects as knocking out HUWE1: it
492 should reduce WNT signaling by promoting GSK3A/GSK3B-dependent phosphorylation and
493 degradation of CTNNB1, and possibly by promoting the second mechanism independent of

494 CTNNB1 stability. Furthermore, since AXIN1 loss in CSNK1A1^{KO} cells eliminated the
495 reduction in WNT signaling caused by HUWE1 loss (Figs 4A-E and Table 1), we reasoned that
496 overexpressing AXIN1 in CSNK1A1^{KO}; HUWE1^{KO} cells should have the opposite effect and
497 synergize with HUWE1 loss to reduce WNT signaling. To test these predictions, we stably
498 overexpressed human AXIN1 in CSNK1A1^{KO} and in CSNK1A1^{KO}; HUWE1^{KO} cells through
499 lentiviral delivery of *AXIN1* cDNA followed by antibiotic selection. We obtained polyclonal cell
500 populations (CSNK1A1^{KO}; AXIN1^{OE} and CSNK1A1^{KO}; HUWE1^{KO}; AXIN1^{OE}, respectively) in
501 which AXIN1 abundance was at least 2-fold higher than that in the respective parental cell lines
502 (S1D Fig).

503 AXIN1 overexpression in CSNK1A1^{KO} cells indeed reduced WNT reporter activity by 80%,
504 which was comparable to the 89% reduction caused by HUWE1 loss in CSNK1A1^{KO} cells (Fig
505 1A). AXIN1 overexpression combined with HUWE1 loss in CSNK1A1^{KO} cells reduced WNT
506 reporter activity by 98%, nearly down to the basal level of unstimulated WT HAP1-7TGP cells
507 (Fig 1A). Therefore, AXIN1 overexpression in CSNK1A1^{KO} cells phenocopied HUWE1 loss,
508 and AXIN1 overexpression in CSNK1A1^{KO}; HUWE1^{KO} cells synergized with HUWE1 loss to
509 reduce WNT signaling. We conclude that HUWE1 and AXIN1 exert opposing effects on WNT
510 signaling.

511 To test whether the reduction in WNT signaling caused by AXIN1 overexpression and by
512 HUWE1 loss was due to the same underlying mechanisms, we measured the abundance of
513 soluble and non-phospho-CTNNB1 in CSNK1A1^{KO}; AXIN1^{OE} and CSNK1A1^{KO}; HUWE1^{KO};
514 AXIN1^{OE} cells, as we had done in WT HAP1-7TGP, CSNK1A1^{KO} and CSNK1A1^{KO};
515 HUWE1^{KO} cells (Figs 1B and 1C, and S1A and S1B Figs). AXIN1 overexpression in
516 CSNK1A1^{KO} cells caused a 45% reduction in soluble CTNNB1 abundance and a 64% reduction

517 in non-phospho-CTNNB1 abundance (Figs 1B and 1C, and S1A and S1B Figs). These
518 reductions were comparable to and greater than the respective 36% and 37% reductions caused
519 by HUWE1 loss in CSNK1A1^{KO} cells (Figs 1B and 1C, and S1A and S1B Figs). AXIN1
520 overexpression combined with HUWE1 loss in CSNK1A1^{KO} cells reduced soluble CTNNB1
521 abundance by 57% and non-phospho-CTNNB1 by 62% (Figs 1B and 1C, and S1A and S1B
522 Figs). These results indicate that HUWE1 and AXIN1 have opposing functions regulating a
523 common mechanism: AXIN1 promotes CTNNB1 phosphodegron phosphorylation and the
524 resulting reduction in CTNNB1 abundance, while HUWE1 antagonizes both.

525 If HUWE1 and AXIN1 exert opposing effects on WNT signaling by regulating the same
526 GSK3A/GSK3B-dependent processes – CTNNB1 phosphorylation and abundance, and
527 potentially another mechanism independent of CTNNB1 stability – then GSK3A/GSK3B
528 inhibition should reverse the effects of AXIN1 overexpression in CSNK1A1^{KO} cells, as it
529 reverses the effects of HUWE1 loss (Figs 1A-C, and S1A and S1B Figs). Therefore, we tested
530 whether the changes in WNT reporter activity, soluble CTNNB1 abundance and CTNNB1
531 phosphodegron phosphorylation caused by AXIN1 overexpression alone or combined with
532 HUWE1 loss were dependent on GSK3A/GSK3B activity. Treatment of CSNK1A1^{KO}; AXIN1^{OE}
533 cells with the GSK3A/GSK3B inhibitor CHIR-99021 reversed the effects of AXIN1
534 overexpression, increasing WNT reporter activity as well as soluble and non-phospho-CTNNB1
535 abundance to levels higher than those measured in DMSO vehicle treated-CSNK1A1^{KO} cells,
536 and comparable to those measured in CHIR-99021-treated CSNK1A1^{KO} cells (Figs 1A-C, and
537 S1A and S1B Figs). GSK3A/GSK3B inhibition with CHIR-99021 also reversed the synergistic
538 reduction in WNT reporter activity, as well as the reduction in soluble and non-phospho-
539 CTNNB1 abundance, caused by combined AXIN1 overexpression and HUWE1 loss in

540 CSNK1A1^{KO} cells (Figs 1A-C, and S1A and S1B Figs). These results demonstrate that in
541 CSNK1A1^{KO} cells, HUWE1 enhances and AXIN1 inhibits WNT signaling by opposing
542 mechanisms mediated by GSK3A/GSK3B. Altogether, our results support the hypothesis that
543 AXIN1, acting as a scaffold in the DC, promotes GSK3A/GSK3B-dependent CTNNB1
544 phosphorylation and degradation, even in the absence of CSNK1A1. HUWE1 enhances WNT
545 signaling by antagonizing this DC activity.

546

547 **Regulation of WNT signaling by HUWE1 requires its ubiquitin ligase activity**

548

549 HUWE1 is a very large 482 kDa ubiquitin ligase with many protein-protein interaction domains
550 in addition to its catalytic HECT domain [27]. Therefore, it was important to determine whether
551 the ubiquitin ligase activity of HUWE1 was required for its functions enhancing WNT signaling.
552 HECT domain ubiquitin ligases form a covalent intermediate between a catalytic cysteine (C)
553 residue in the HECT domain and ubiquitin before ubiquitin is transferred to the substrate [28].
554 We used CRISPR-mediated base editing [29] to engineer the endogenous *HUWE1* locus of
555 CSNK1A1^{KO} cells, introducing a single point mutation that replaced the catalytic C4341 residue
556 with arginine (R). We isolated three independent clonal cell lines (CSNK1A1^{KO}; HUWE1^{C4341R-1},
557 CSNK1A1^{KO}; HUWE1^{C4341R-2} and CSNK1A1^{KO}; HUWE1^{C4341R-3}) in which we confirmed by
558 sequencing that the intended point mutation had been introduced (S1 File). We compared the
559 effects of eliminating the catalytic activity of HUWE1 to those of knocking out HUWE1 on
560 WNT signaling. All three CSNK1A1^{KO}; HUWE1^{C4341R} clonal cell lines exhibited a substantial
561 89-94% reduction in WNT reporter activity and a 79-88% reduction in the expression of three
562 WNT target genes, equivalent to what we observed in CSNK1A1^{KO}; HUWE1^{KO} cells (Figs 5A-

563 D). The C4341R point mutation did not affect HUWE1 protein stability as determined by
564 Western blot analysis of the three CSNK1A1^{KO}; HUWE1^{C4341R} cell lines (Fig 5E). In contrast, no
565 HUWE1 protein was detected in CSNK1A1^{KO}; HUWE1^{KO} cells (Fig 5E). Therefore, the
566 reduction in WNT signaling measured in CSNK1A1^{KO}; HUWE1^{C4341R} cells was not due to loss
567 of HUWE1 protein, but rather due to the elimination of its catalytic activity. We conclude that
568 the ubiquitin ligase activity of HUWE1 is required for its functions enhancing WNT signaling.
569

570 **Discussion:**

571

572 In this study we probed the mechanisms underlying the requirement for the HECT domain
573 ubiquitin ligase HUWE1 to sustain hyperactive WNT/CTNNB1 signaling [15]. We demonstrate
574 that HUWE1 enhances WNT/CTNNB1 signaling through two distinct mechanisms: by
575 antagonizing DC-mediated CTNNB1 phosphorylation and degradation, and through another
576 mechanism independent of CTNNB1 stability. These results are significant for two main reasons.
577 First, they reveal a new mechanism that controls CTNNB1 stability, the main regulated step in
578 WNT/CTNNB1 signaling. Second, by controlling another downstream step in the pathway,
579 HUWE1 adds a new layer of regulation superimposed on the core WNT/CTNNB1 signaling
580 module. Importantly, the coordinated regulation of CTNNB1 abundance and an independent
581 signaling step in the pathway by HUWE1 would be an efficient way to control multiple
582 processes that determine WNT signaling output. This may enable sensitive and robust activation
583 of the pathway.

584 In CSNK1A1^{KO} cells, GSK3A/GSK3B still phosphorylate a fraction of CTNNB1 at residues
585 S33, S37 and T41 in the phosphodegron, which reduces CTNNB1 abundance (Fig 1). HUWE1
586 enhances signaling by counteracting DC-dependent phosphorylation of these residues, since
587 HUWE1 loss in CSNK1A1^{KO} cells increases phosphorylation and reduces both CTNNB1
588 abundance and WNT signaling activity (Fig 1). However, the reduction in CTNNB1 abundance
589 caused by HUWE1 loss appears insufficient to account for the larger reduction in WNT target
590 gene expression (Fig 1), suggesting that HUWE1 also enhances WNT/CTNNB1 signaling
591 through another mechanism. In CTNNB1^{ST-A} cells containing mutations in the CTNNB1
592 phosphodegron that render CTNNB1 abundance insensitive to regulation by WNT ligands and

593 the DC, HUWE1 enhances WNT target gene expression through a mechanism distinct from the
594 control of CTNNB1 stability (Fig 2). Furthermore, regulation of WNT/CTNNB1 signaling by
595 HUWE1 is mediated by a subset of DC components, including APC, AXIN1 and GSK3A or
596 GSK3B, but excluding CSNK1A1 and AXIN2 (Figs 1, 3 and 4). HUWE1 promotes WNT
597 signaling by antagonizing the activity of this DC (Fig 1). The ubiquitin ligase activity of
598 HUWE1 is required to enhance WNT signaling (Fig 5), suggesting that a substrate of HUWE1
599 mediates its function.

600 One of the mechanisms whereby HUWE1 enhances WNT/CTNNB1 signaling is by
601 antagonizing phosphorylation of the CTNNB1 phosphodegron by the DC complex, thereby
602 increasing CTNNB1 abundance, but surprisingly this happens in the absence of CSNK1A1.
603 These results demonstrate that in HAP1 cells, CSNK1A1 is not absolutely required for
604 GSK3A/GSK3B-dependent phosphorylation of residues S33, S37 and T41 in the CTNNB1
605 phosphodegron, either because GSK3A/GSK3B can phosphorylate these residues without the
606 priming phosphorylation of S45 by CSNK1A1, or because other kinases phosphorylate S45 in
607 the absence of CSNK1A1. While priming of S45 by CSNK1A1 is generally considered a
608 requirement for phosphorylation of S33, S37 and T41 by GSK3A/GSK3B [6, 7], some reports
609 suggest it is not [30, 31].

610 We also show there is another mechanism whereby HUWE1 enhances WNT/CTNNB1
611 signaling that is independent of CTNNB1 stability. HUWE1 could potentially regulate CTNNB1
612 subcellular localization or its interactions with the TCF/LEF transcription complex, or it could
613 regulate other downstream steps in the pathway. Elucidating this second mechanism and whether
614 it is also mediated by a subset of DC complex components, like HUWE1-dependent regulation

615 of CTNNB1 abundance, will be crucial to understand the full scope of how HUWE1 regulates
616 WNT signaling.

617 Intriguingly, only a subset of DC components, including APC, AXIN1 and GSK3A or
618 GSK3B, but not CSNK1A1 or AXIN2, mediate the function of HUWE1 in WNT signaling (Figs
619 1, 3 and 4). We were surprised to find that AXIN1 was required to mediate the effects of
620 HUWE1 but AXIN2 was not. In WT HAP1-7TGP cells, AXIN1 and AXIN2 are redundant in
621 their capacity to suppress WNT signaling: eliminating either AXIN1 or AXIN2 has no effect on
622 WNT reporter activity, whereas eliminating both results in constitutive pathway activation [15].
623 Yet, in CSNK1A1^{KO} cells, only AXIN1 loss eliminated the reduction in WNT target gene
624 expression caused by HUWE1 KD (Fig 4 and Table 1). These results suggest that AXIN1 and
625 AXIN2 are not redundant in their capacity to mediate the effects of HUWE1, at least in the
626 absence of CSNK1A1. This finding is unexpected given that mouse AXIN1 and AXIN2 proteins
627 have been reported to be functionally equivalent *in vivo* [32], and will require further
628 investigation.

629 The ubiquitin ligase activity of HUWE1 is required to promote WNT signaling in
630 CSNK1A1^{KO} cells (Fig 5). What are the relevant ubiquitylated HUWE1 substrates, and how do
631 they regulate WNT signaling? Does HUWE1-dependent ubiquitylation target putative substrates
632 for proteasomal degradation or does it regulate their activity? Since a subset of DC components
633 mediates the effects of HUWE1 on WNT signaling, is the abundance or activity of a DC
634 component regulated by HUWE1-dependent ubiquitylation or are there other ubiquitylated
635 substrates that indirectly impinge on DC abundance or activity? Identification of the relevant
636 HUWE1 substrates should help answer these questions.

637 Previous reports have implicated HUWE1 as a *negative* regulator of WNT signaling [33-36].
638 This is the opposite of what we find in WT HAP1-7TGP, CSNK1A1^{KO} and CTNNB1^{ST-A} cells,
639 in which HUWE1 is a *positive* regulator of the pathway: eliminating HUWE1 or its catalytic
640 activity in these cells substantially reduces WNT/CTNNB1 signaling (Figs 1-5). HUWE1 has
641 been reported to polyubiquitylate DVL and prevent DVL multimerization [33], which is required
642 to form a functional signalosome and transduce WNT signals [37, 38]. HUWE1 has also been
643 reported to ubiquitylate CTNNB1 and promote CTNNB1 degradation [34]. The latter mechanism
644 is in fact the opposite of what we find in CSNK1A1^{KO} cells, in which HUWE1 loss reduces
645 CTNNB1 abundance (Fig 1). Based on both reported mechanisms, HUWE1 loss would be
646 expected to promote rather than reduce WNT signaling. Therefore, we do not think that DVL or
647 CTNNB1 are the relevant ubiquitylated substrates that mediate the effects of HUWE1 on WNT
648 signaling in HAP1 cells. These disparate results could reflect differences in experimental
649 systems, since the previous reports primarily studied HUWE1 in *C. elegans* and HEK293T cells
650 [33, 34], while the experiments presented in the current study were conducted in HAP1 cells.
651 Identifying the substrate of HUWE1 that mediates its role as a positive regulator of
652 WNT/CTNNB1 signaling in HAP1 cells should help explain these differences.

653 We demonstrate that HUWE1 loss reduces WNT signaling in cells containing mutations in
654 some WNT pathway components but not in others (Figs 1-5). These results raise the possibility
655 of targeting the signaling mechanisms by which HUWE1 enhances WNT signaling selectively in
656 tumors harboring mutations in specific WNT pathway components. Eliminating or reducing the
657 activity of HUWE1 itself, which reduces WNT/CTNNB1 signaling in WT HAP1-7TGP,
658 CSNK1A1^{KO} and CTNNB1^{ST-A} cells, is unlikely to be a viable therapeutic strategy due to the
659 pleiotropic effects of HUWE1 on cell physiology, including tumor suppressor functions [39].

660 However, if the relevant ubiquitylated target of HUWE1 is identified, there may be other ways to
661 phenocopy the effects of HUWE1 loss on WNT signaling more specifically. Phenocopying the
662 effects of HUWE1 loss may not be effective in tumors driven by APC truncations, given that in
663 APC^{KO} cells HUWE1 loss does not reduce WNT signaling due to the role of APC itself in
664 mediating the effects of HUWE1. However, in tumors containing activating mutations in
665 CTNNB1 like those engineered into our CTNNB1^{ST-A} cell line, or mutations in the ZNRF3 or
666 RNF43 tumor suppressors, all of which result in hyperactive WNT signaling in the presence of a
667 functional DC, phenocopying the effects of HUWE1 loss may reduce WNT signaling enough to
668 provide a therapeutic benefit.

669 We recognize that all the experiments presented in the Results section of this manuscript
670 were conducted in HAP1 cells or derivatives thereof, which could raise concerns about the
671 generality and specificity of our conclusions. We also studied HUWE1 in other cell lines
672 commonly used in WNT signaling research, but our attempts to knock out HUWE1 yielded only
673 partial KOs. We targeted *HUWE1* by CRISPR/Cas9-mediated genome editing in HEK293T-7TG
674 and HEK293T-7TG CSNK1A1^{KO} cells (see Materials and methods). Out of 113 independent
675 clonal cell lines in which we identified mutations in all *HUWE1* alleles, at least one allele had
676 been repaired in frame to encode WT HUWE1 protein (S6A and S6B Figs). This is probably
677 because HUWE1 is a common essential gene as per DEPMap classification
678 (<https://depmap.org/portal/gene/HUWE1?tab=overview>), so complete loss of HUWE1 may be
679 lethal in HEK293T cells. However, we have previously shown that microinjection of *HUWE1*
680 mRNA into *Xenopus* embryos results in body axis duplication [15], consistent with a more
681 general role of HUWE1 as a positive regulator of WNT signaling beyond HAP1 cells.
682 Furthermore, we designed many of our experiments so as to minimize the possibility of non-

683 specific or pleiotropic effects. We knocked out HUWE1 in two independent CSNK1A1^{KO} cell
684 lines with comparable results (Fig 3). We used two different sgRNAs for CRISPR/Cas9-
685 mediated HUWE1 KO in multiple clonal cell lines (Figs 1-3), a different sgRNA for CRISPR
686 base editing of the HUWE1 catalytic residue in multiple CSNK1A1^{KO}; HUWE1^{C4341R} clonal cell
687 lines (Fig 5), and another two different sgRNAs for CRISPRi-mediated HUWE1 KD in
688 polyclonal cell populations (Fig 4). In all cases, we found reproducible reductions in
689 WNT/CTNNB1 signaling. We also saw consistent effects of HUWE1 loss in three different
690 genetic backgrounds: WT HAP1-7TGP, CSNK1A1^{KO} and CTNNB1^{ST-A} cells (Figs 1-5). We
691 measured the effects of HUWE1 loss on three or four endogenous WNT target genes and on an
692 7TGP, an established WNT transcriptional reporter, with comparable outcomes (Figs 1-5). The
693 effects of HUWE1 on WNT signaling could be reversed completely by a relatively short and
694 specific pharmacological treatment with the GSK3A/GSK3B inhibitor CHIR-99021 (Fig 1), and
695 by introducing mutations in some DC components but not others (Figs 3 and 4). Altogether,
696 these results make it very unlikely that the effects of HUWE1 loss are non-specific or due to
697 pleiotropic downregulation of unrelated cellular functions that affect WNT signaling.

698 Our study also highlights the remarkable potential of HAP1 haploid cells to dissect complex
699 genetic networks in a cell line of human origin [16] through a combination of genome-wide
700 forward genetic screens, loss-of-function and site-directed mutagenesis analyses, and genetic
701 interaction analyses. Despite great advances in CRISPR/Cas-based genome editing technologies
702 during the last decade [40], it remains challenging to knock out two or more alleles of multiple
703 genes and to introduce targeted homozygous point mutations at scale in diploid primary cells,
704 stem cells, and polyploid immortalized cell lines. We could readily do both in HAP1 cells
705 because they have a single allele of most genes. This enabled us to conduct loss-of-function

706 genetic analyses in multiple genetic backgrounds by comparing several HUWE1 KO and control
707 WT clonal cell lines to obtain highly quantitative phenotypic data that confirmed and extended
708 the results of our initial genetic screens (Fig 3). Using CRISPR/Cas9-mediated HDR, we
709 generated a CTNNB1 variant in which we mutated three key phosphorylation sites in the
710 phosphodegron at the single endogenous *CTNNB1* locus, and in a second round of
711 CRISPR/Cas9-mediated genome editing we generated multiple HUWE1 KO and WT cell lines
712 to demonstrate that regulation of WNT signaling by HUWE1 has a component that is
713 independent of CTNNB1 stability (Fig 2). Using CRISPR-mediated base editing, we generated
714 three clonal cell lines containing a point mutation in the catalytic residue of HUWE1 at the single
715 endogenous *HUWE1* locus, which enabled us to demonstrate that the ubiquitin ligase activity of
716 HUWE1 is required for its function in WNT signaling (Fig 5). Finally, we generated single,
717 double, and triple KO mutants for all components of the DC, alone and in certain combinations
718 (11 distinct mutant genetic backgrounds in total) (Table 1 and S4 Fig). Combined with a
719 CRISPRi strategy, this enabled us to carry out an extensive genetic interaction analysis and
720 demonstrate that positive regulation of WNT signaling by HUWE1 is mediated by a subset of
721 DC components (Fig 4 and Table 1). These kinds of genetic analyses would have been
722 practically impossible to conduct in any diploid or polyploid human cell line. We hope this study
723 will inspire other researchers to take advantage of haploid human cell lines, of which there are
724 now many available [41, 42], to unravel other signaling pathways or biological processes in
725 similar ways.

726 HUWE1 has emerged as an important ubiquitin ligase with many cellular functions [17-20].
727 Here we show another role for HUWE1 regulating WNT/CTNNB1 signaling. Regulation of
728 CTNNB1 abundance by the DC is the central step in WNT/CTNNB1 signaling. Our discovery

729 that HUWE1 enhances WNT signaling by antagonizing DC-dependent CTNNB1
730 phosphorylation, thereby increasing CTNNB1 abundance, demonstrates that this crucial step in
731 WNT/CTNNB1 signaling is subject to more nuanced regulation than previously thought. The
732 second mechanism by which HUWE1 enhances WNT signaling independently of CTNNB1
733 stability is an intriguing additional layer of regulation that remains to be elucidated. Both
734 mechanisms provide new insights into WNT signaling and ubiquitin biology, bridging two
735 research fields that already have many intimate connections.
736

737 **Materials and methods:**

738

739 The following Materials and methods relevant to this manuscript have been described previously
740 [15]: cell lines and growth conditions, preparation of WNT3A conditioned media and
741 construction of the HAP1-7TGP WNT reporter haploid cell line.

742

743 **Tissue culture media**

744 Complete growth medium (CGM) 1 contains Dulbecco's Modified Eagles Medium (DMEM)
745 with High Glucose, without L-Glutamine and Sodium Pyruvate (GE Healthcare Life Sciences
746 Cat. # SH30081.01); 1X GlutaMAX-I (Thermo Fisher Scientific Cat. # 35050079); 1X MEM
747 Non-Essential Amino Acids (Thermo Fisher Scientific Cat. # 11140050); 1 mM Sodium
748 Pyruvate (Thermo Fisher Scientific Cat. # 11360070); 40 Units/ml Penicillin, 40 mg/ml
749 Streptomycin (Thermo Fisher Scientific Cat. # 15140122); 10% Fetal Bovine Serum (FBS).

750 CGM 2 contains Iscove's Modified Dulbecco's Medium (IMDM) with L-glutamine, with
751 HEPES, without Alpha-Thioglycerol (GE Healthcare Life Sciences Cat. # SH30228.01); 1X
752 GlutaMAX-I; 40 Units/ml Penicillin, 40 mg/ml Streptomycin; 10% FBS.

753

754 **Plasmids**

755 pX330-U6-Chimeric_BB-CBh-hSpCas9 (pX330) (Addgene plasmid # 42230) was a gift from
756 Feng Zhang; pCMV_ABEmax_P2A_GFP (Addgene plasmid # 112101) was a gift from David
757 Liu; MLM3636 (Addgene plasmid # 43860) was a gift from Keith Joung; Lenti-(BB)-EF1a-
758 KRAB-dCas9-P2A-BlastR (Addgene plasmid # 118154) was a gift from Jorge Ferrer;
759 LentiCRISPRv2-mCherry (Addgene plasmid # 99154) was a gift from Agata Smogorzewska;

760 pMDLg/pRRE (Addgene plasmid # 12251), pRSV-Rev (Addgene plasmid # 12253) and
761 pMD2.G (Addgene plasmid # 12259) were a gift from Didier Trono; pCS2-YFP was a gift from
762 Henry Ho; pmCherry was a gift from Jan Carette; pX458-mCherry was generated as described
763 previously [43].

764 The following plasmids were purchased: pLenti6.2/V5-DEST (Thermo Fisher Scientific Cat.
765 # V36820); pENTR2B (Thermo Fisher Scientific Cat. # A10463); MGC Human AXIN1
766 Sequence-verified cDNA (Clone ID 5809104) (Horizon Cat. # MHS6278-202833071).

767 To generate pCMV_ABEmax_P2A_mCherry, mCherry was amplified by PCR from plasmid
768 pmCherry using primers pCMV_ABEmax_P2A_mCherry_Fw (5'-GAA GCA GGC TGG AGA
769 CGT GGA GGA GAA CCC TGG ACC TAT GGT GAG CAA GGG CGA GGA-3') and
770 pCMV_ABEmax_P2A_mCherry_Rv (5'-CAG ACT TGT ACA GCT CGT CCA TGC CG-3'),
771 designed to include BsmBI and BsrGI restriction sites, respectively. The PCR product was
772 digested with BsmBI and BsrGI and ligated into pCMV_ABEmax_P2A_GFP digested with the
773 same enzymes to replace GFP with mCherry.

774 To generate pLenti6.2-V5-EXP-N-TERM-S-FLAG-N-hAXIN1, human AXIN1 was
775 amplified by PCR from MGC Human AXIN1 Sequence-verified cDNA (Clone ID 5809104)
776 using primers pENTR2B_SalI_S-FLAG-N_hAXIN1_pcr_fw (5'-GCG CCG GAA CCA ATT
777 CAG TCG ACC CTG CAG GAT GGA TTA CAA GGA CGA CGA TGA CAA GGG CGG
778 CCG CAT GAA TAT CCA AGA GCA GGG TTT CCC CTT GGA CC-3'), containing an N-
779 terminal SalI restriction site followed by a FLAG tag sequence flanked by SbfI and NotI
780 restriction sites, and pENTR2B_XhoI_hAXIN1_pcr_rv (5'-AAA GCT GGG TCT AGA TAT
781 CTC GAG TCA GTC CAC CTT CTC CAC TTT GCC GAT GA-3'), containing a C-terminal
782 XhoI restriction site. The product was digested with SalI and XhoI, and subcloned into

783 pENTR2B digested with the same enzymes. One clone was sequenced completely and subcloned
784 into pLenti6.2/V5-DEST using the Gateway LR Clonase II Enzyme mix.

785 All constructs were confirmed by sequencing.

786

787 **Antibodies**

788 Primary antibodies: purified mouse anti- β -catenin (Clone 14/Beta-Catenin) (1:1000, BD
789 Biosciences Cat. # 610154), rabbit mAb anti-non-phospho (active) β -catenin (Ser33-37-Thr41)
790 (D13A1) (1:1000, Cell Signaling Technology Cat. # 8814), mouse anti-GAPDH (1:4000, Santa
791 Cruz Biotechnology, Cat. # sc-47724), recombinant rabbit anti-Sodium Potassium (Na^+/K^+)
792 ATPase [EP1845Y] (1:4000, Abcam Cat. # ab76020), rabbit anti-Las1/Urb1 (HUWE1)
793 (1:1000, Bethyl Laboratories Cat. # A300-486A), rabbit mAb anti-AXIN1 (C76H11) (1:1000,
794 Cell Signaling Technology Cat. # 2087), rabbit mAb anti-AXIN2 (76G6) (1:500, Cell Signaling
795 Technology Cat. # 2151), rabbit mAb anti-GSK-3 α/β (D75D3) (1:2000, Cell Signaling
796 Technology Cat. # 5676), mouse anti-APC (NT, clone Ali 12.28) (1:1000, Millipore Sigma, Cat.
797 # MAB3785), rabbit anti-APC (1:1000, Biorbyt Cat. # orb213564), mouse anti-CSNK1A1
798 (1:250, Santa Cruz Biotechnology, Cat. # sc-74582).

799 Secondary antibodies: IRDye 800CW donkey anti-mouse IgG (H+L) (1:10000, Li-Cor Cat. #
800 926-32212), IRDye 680RD donkey anti-rabbit IgG (H+L) (1:10000, Li-Cor Cat. # 925-68073),
801 peroxidase AffiniPure donkey anti-goat IgG (H+L) (1:5000, Jackson ImmunoResearch
802 Laboratories Cat. # 705-035-003), peroxidase AffiniPure goat anti-rabbit IgG (H+L) (1:10000,
803 Jackson ImmunoResearch Laboratories Cat. # 111-035-003), peroxidase AffiniPure donkey anti-
804 mouse IgG (H+L) (1:5000, Jackson ImmunoResearch Laboratories Cat. # 715-035-150), goat
805 anti-mouse IgG (H+L) HRP conjugate (1:10000, Bio-Rad Cat. # 1706516).

806 Primary and secondary antibodies used for detection with the Li-Cor Odyssey imaging
807 system were diluted in a 1 to 1 mixture of Odyssey Intercept Blocking Buffer (Li-Cor Cat. #
808 927–40000) and TBST (Tris buffered saline (TBS) + 0.1% Tween-20), and those used for
809 detection by chemiluminescence were diluted in TBST + 5% skim milk. All primary antibody
810 incubations were done overnight at 4°C, and secondary antibody incubations were done for 1 hr
811 at room temperature (RT).

812

813 **Construction of mutant HAP1-7TGP cell lines by CRISPR/Cas9-mediated genome editing**

814 Oligonucleotides encoding single guide RNAs (sgRNAs) (S2 File) were selected from a
815 published library [44], or designed using either of two online CRISPR design tools [45, 46] and
816 cloned into either pX330 or pX458-mCherry according to a published protocol [47].

817 Clonal HAP1-7TGP cell lines were established by transient transfection with either pX330 or
818 pX458-mCherry containing the sgRNA followed by single cell sorting as follows. A transfection
819 mix was prepared by diluting 450 ng of pX330 and 50 ng of pmCherry (used as a cotransfection
820 marker for FACS sorting) or 500 ng of pX458-mCherry in 48 µl Opti-MEM I, adding 2 µl of X-
821 tremeGENE HP and incubating for 20 min at RT. HAP1-7TGP cells or derivatives thereof were
822 reverse-transfected in a well of a 24-well plate by overlaying 0.5 ml of CGM 2 (without
823 antibiotics) containing 6×10^5 cells over the 50 µl of transfection mix. Cells were passaged to a
824 10 cm dish ~24 hr post-transfection, using 150 µl of Trypsin-EDTA (0.25%) (Thermo Fisher
825 Scientific Cat. # 25200056) to detach them (reverse-transfection of HAP1 cells caused unusually
826 high adherence, hence the higher trypsin concentration). Three to four days post-transfection,
827 single transfected (mCherry⁺) cells were sorted into 96-well plates containing 200 µl of CGM 2

828 per well and grown undisturbed for 16 to 18 days. Single colonies were passaged to 24-well
829 plates, and a small number of cells was reserved for genotyping.

830 For genotyping, genomic DNA was extracted by adding 4 volumes of QuickExtract DNA
831 Extraction Solution (Epicentre Cat. # QE09050) to the cells. Extracts were incubated 10 min at
832 65°C, 3 min at 98°C, and 5 µl were used as input for PCR amplification of the genomic locus
833 containing the sgRNA target site in 15 µl reactions containing 1X LongAmp Taq reaction buffer,
834 300 mM of each dNTP, 400 nM of each of the flanking primers indicated in S2 File (most of
835 them designed using the Primer-BLAST online tool from the NCBI) and 0.1 units/µl of
836 LongAmp Taq DNA polymerase (NEB Cat. # M0323L). Amplification of the genomic locus
837 containing the sgRNA target site was confirmed by analysis of the PCR products on a 1%
838 agarose gel and the presence of desired mutations was confirmed by sequencing the amplicons
839 using the primers indicated in S2 File. Given that most engineered cell lines remained haploid,
840 sequencing results were usually unequivocal. Sequencing results for all the clonal cell lines used
841 in the study is presented in S1 File, and for selected clonal cell lines, immunoblot analysis
842 confirmed the absence of the protein products.

843 Whenever possible, multiple independent mutant cells lines, often generated using two
844 different sgRNAs (see S1 File), were expanded and used for further characterization. For some
845 of the comparisons between WT and mutant cells, multiple individual cell lines confirmed by
846 sequencing to be WT at the sgRNA target site were also expanded and used as controls. To
847 generate double and triple mutant cell lines, a single clonal cell line with the first desired
848 mutation was used in a subsequent round of transfection with either pX330 or pX458-mCherry
849 containing the second and, if applicable, third sgRNAs. Alternatively, WT HAP1-7TGP cells

850 were directly transfected with a combination of pX330 or pX458-mCherry constructs targeting
851 two genes simultaneously.

852

853 **Construction of CTNNB1^{ST-A} cell line by CRISPR/Cas9-mediated HDR**

854 Oligonucleotides encoding sgRNAs complementary to exon 3 of *CTNNB1* (S2 File) were
855 designed using either of two online CRISPR design tools [45, 46] and cloned into pX458-
856 mCherry using a published protocol [47].

857 Clonal CTNNB1^{ST-A} cell lines were established by transient transfection of HAP1-7TGP
858 cells with pX458-mCherry containing the sgRNA, and a single stranded oligonucleotide
859 (ssODN) donor template encoding the desired mutations, called CTNNB1 (ST-A mutant) donor
860 (5'-ATT TGA TGG AGT TGG ACA TGG CCA TGG AAC CAG ACA GAA AAG CGG CTG
861 TTA GTC ACT GGC AGC AAC AGT CTT ACC TGG ACG CTG GAA TCC ATG CTG GTG
862 CCA CTG CCA CAG CTC CTG CTC TGA GTG GTA AAG GCA ATC CTG AGG AAG
863 AGG ATG TGG ATA CCT CCC AAG TCC TGT ATG AGT GGG AAC AGG GAT TTT CTC
864 AG-3'). A transfection mix was prepared by diluting 500 ng pX458-mCherry-CTNNB1-Ex3-
865 sgRNA and 500 ng (8 pmol) ssODN in 48 μ l Opti-MEM I. 2 μ l of X-tremeGENE HP were
866 added, and the mix was vortexed and incubated for 20 min at RT. The 50 μ l mix was placed in
867 an empty well of a 24-well plate and 0.5 ml of CGM 2 containing 6×10^5 cells was seeded onto
868 the mix. The cells were passaged the following day to a 10 cm dish and grown for 3 additional
869 days. Single cells exhibiting high EGFP fluorescence from the 7TGP WNT reporter, presumably
870 due to successful mutagenesis of the CTNNB1 phosphodegrom, were sorted, expanded, and
871 genotyped as described above. A single clonal cell line containing point mutations in three of the

872 four targeted sites in the phosphodegron (S2A Fig and S1 File) was used for all subsequent
873 experiments.

874

875 **Construction of HUWE1 catalytic mutant CSNK1A1^{KO}; HUWE1^{C4341R} cell lines by base**
876 **editing**

877 An oligonucleotide encoding an sgRNA complementary to exon 83 of *HUWE1* (S2 File) was
878 designed to include the targeted nucleotide within the editing window of the base editor
879 ABEmax (positions 4-8 in the protospacer) using BE-Hive (<https://www.crisprbehive.design>), an
880 online base editing sgRNA design tool [48], and cloned into MLM3636 according to a published
881 protocol (Joung Lab gRNA cloning protocol:

882 https://media.addgene.org/data/plasmids/43/43860/43860-attachment_T35tt6ebKxov.pdf). A
883 transfection mix was prepared by diluting 750 ng pCMV-ABEmax-P2A-mCherry and 250 ng
884 MLM3636-HUWE1-C4341R-sgRNA1 in 50 μ l Opti-MEM I, adding 2 μ l of X-tremeGENE HP
885 and incubating for 20 min at RT. CSNK1A1^{KO} cells were reverse-transfected in a well of a 24-
886 well plate by overlaying 0.5 ml of CGM 2 (without antibiotics) containing 6×10^5 cells over the
887 50 μ l of transfection mix. Cells were passaged to a 6 cm dish ~24 hr post-transfection, using 150
888 μ l of Trypsin-EDTA (0.25%) (Thermo Fisher Scientific Cat. # 25200056) to detach them. Three
889 days post-transfection, single transfected (mCherry⁺) cells were sorted into 96-well plates
890 containing 200 μ l of CGM 2 per well and grown undisturbed for 16 to 18 days. Cells were
891 expanded and genotyped as described above.

892

893 **Targeting *HUWE1* by CRISPR/Cas9 in HEK293T-7TG and HEK293T-7TG CSNK1A1^{KO}**
894 **cells**

895 Oligonucleotides HUWE1-IVT-2503-F and HUWE1-IVT-2503-R encoding sgRNAs
896 complementary to exon 6 of *HUWE1* (S2 File) were designed using sgRNA Scorer 2.0 [49] and
897 cloned into LentiCRISPRv2-mCherry previously digested with BsmBI. HEK293T-7TG is a
898 clonal cell line derived from HEK293T cells that contains a fluorescent WNT reporter.
899 HEK293T-7TG CSNK1A1^{KO} is a clonal cell line derived from HEK293T-7TG cells in which
900 CSNK1A1 has been knocked out. Construction of both cell lines will be described elsewhere.

901 Clonal HEK293T-7TG and HEK293T-7TG CSNK1A1^{KO} cell lines in which HUWE1 was
902 targeted by CRISPR/Cas9 were established by transient transfection with LentiCRISPRv2-
903 mCherry containing the sgRNAs followed by single cell sorting. ~24 hr before transfection, 8 x
904 10⁴ HEK293T-7TG or HEK293T-7TG CSNK1A1^{KO} cells per well were seeded in 24-well plates
905 and grown in CGM 1. On the day of transfection, CGM 1 was replaced with 450 µl of antibiotic-
906 free CGM 1. 50 µl of a transfection mixture containing 500 ng LentiCRISPRv2-mCherry and 1
907 µl of X-tremeGENE™ HP DNA Transfection Reagent (Millipore Sigma, Cat # 06366236001)
908 prepared in OptiMEM were added dropwise. ~24 hr post-transfection, cells were transferred to a
909 6 cm dish, and ~72 hr post-transfection, single transfected (mCherry⁺) cells were sorted into 96-
910 well plates containing 200 µl of CGM 1 media per well and grown undisturbed for 16 days.
911 Single colonies were expanded by passaging to 24-well plates, and 10 µl of cell suspension were
912 reserved for genotyping.

913 For genotyping, genomic DNA was extracted by adding 4 volumes of QuickExtract DNA
914 Extraction Solution (Epicentre, Cat # QE09050) to the cells. Extracts were incubated for 10 min
915 at 65°C, 3 min at 98°C, and 5 µl were used as input for PCR amplification of the *HUWE1* target
916 site in 15 µl reactions containing 1X LongAmp Taq reaction buffer, 300 mM of each dNTP, 400
917 nM of each of the flanking primers PS1057-NGS-F and PS1057-NGS-R (S2 File) and 0.1

918 units/ μ l of LongAmp Taq DNA polymerase (NEB Cat. # M0323L). In a second amplification
919 step, complete Illumina adapter sequences (F: 5'-AAT GAT ACG GCG ACC ACC GAG ATC
920 TAC AC <8 bp barcode> AC ACT CTT TCC CTA CAC GAC GCT CTT CCG ATC* T-3' ; R:
921 5'-CAA GCA GAA GAC GGC ATA CGA GAT <8 bp barcode> G TGA CTG GAG TTC AGA
922 CGT GTG CTC TTC CGA TC*T-3'; * indicates a phosphorothioate (PTO) linked base) were
923 added and the amplicons were sequenced on the MiSeq system (Illumina). FASTQ sequencing
924 files were analyzed using the branch 1.1 version [50] of a previously described analysis pipeline
925 (https://github.com/rajchari2/ngs_amplicon_analysis). Total (dark blue) and out-of-frame (light
926 blue) mutation rates were calculated and plotted (S6 Fig).

927

928 **Preparation of lentivirus, lentiviral transduction, and selection of HUWE1 KD and AXIN1-** 929 **overexpressing polyclonal cell populations**

930 The transfer plasmid used to generate HUWE1 KD cell lines by CRISPRi was Lenti-(BB)-EF1a-
931 KRAB-dCas9-P2A-BlastR. The transfer plasmid used to generate cell lines overexpressing
932 AXIN1 was pLenti6.2-V5-EXP-N-TERM-S-FLAG-N-hAXIN1. ~24 hr before transfection, 21 x
933 10⁶ HEK293T cells were plated in 20 ml of CGM 1 without antibiotics in a T-175 flask. A
934 transfection mixture was prepared by diluting 9.3 μ g of transfer plasmid, 7 μ g of pMDLg/pRRE,
935 7 μ g of pRSV-Rev, 4.66 μ g of pMD2.G, 1.05 μ g pCS2-YFP (as a cotransfection marker), and
936 87.15 μ l of 1 mg/ml polyethylenimine (PEI) in a final volume of 1 ml serum-free DMEM. The
937 mixture was incubated for 20 min at RT and added to the culture media in the flasks. The day
938 after transfection, the media was replaced with 18 ml of CGM1 containing a total of 20% FBS
939 without antibiotics. ~48 hr after transfection, the media was collected (first viral harvest),
940 centrifuged at 1000 x g for 5 min to remove cell debris, and the supernatant was reserved at 4°C.

941 18 ml of fresh media were added to the flask of cells. ~72 hr after transfection, the media was
942 collected (second viral harvest), centrifuged as before, and the supernatant was pooled with the
943 first viral harvest. The pooled supernatant was filtered through 0.45 μm filters (Acrodisc syringe
944 filters with 0.45 μm Supor membrane, Pall Corporation Cat. # 4654). The filtered media
945 containing lentiviral particles was aliquoted, snap frozen in liquid nitrogen, and stored at -80°C .

946 For smaller scale preparations of the lentivirus used for AXIN1 overexpression, the above
947 protocol was followed but the lentivirus was prepared using 293FT cells in in T-25 flasks and all
948 quantities and volumes were scaled down by $\sim 1/7$. 3×10^6 293FT cells were plated in 5 ml of
949 CGM 1 without antibiotics in a T-25 flask. A transfection mixture was prepared by diluting 1.33
950 μg of transfer plasmid, 1 μg of pMDLg/pRRE, 1 μg of pRSV-Rev, 0.66 μg of pMD2.G, 0.15 μg
951 pCS2-YFP (as a cotransfection marker), and 69.4 $\mu\text{g}/\text{ml}$ PEI in a final volume of 180 μL serum-
952 free DMEM. The mixture was incubated for 20 min at RT and added to the culture media in the
953 flasks. The day after transfection, the media was replaced with 2.5 ml of CGM 1 containing 20%
954 FBS without antibiotics and the viral supernatants were collected and processed as described
955 above.

956 Approximately 24 hr before transduction, 2.5×10^5 HAP1-7TGP cells or derivatives thereof
957 were seeded in a 6-well plate. Cells were transduced by adding 1 ml of lentivirus-containing
958 supernatant mixed with 1 ml of CGM 2 and 4.4 $\mu\text{g}/\text{ml}$ polybrene. ~24 hr post-transduction, cells
959 were passaged to 10 cm dishes and selected with 8 $\mu\text{g}/\text{ml}$ blasticidin in CGM 2 for ~96 hr.
960 Untransduced cells from each genetic background were treated in parallel with 8 $\mu\text{g}/\text{mL}$
961 blasticidin to ensure that all cells were killed by the time selection of transduced cells was
962 complete.

963

964 **Analysis of WNT reporter fluorescence**

965 To measure WNT reporter activity in HAP1-7TGP cells or derivatives thereof, ~24 hr before
966 treatment cells were seeded in 24-well plates at a density of 8×10^4 per well and grown in 0.5 ml
967 of CGM 2. Cells were treated for 24 hr with the indicated concentrations of WNT3A CM diluted
968 in CGM 2. Cells were washed with 0.5 ml PBS, harvested in 150 μ l of Trypsin-EDTA (0.05%)
969 (Thermo Fisher Scientific Cat. # 25300054), resuspended in 450 μ l of CGM 2, and EGFP
970 fluorescence was measured by FACS on either a SA3800 Spectral Cell Analyzer (Sony
971 Biotechnology) or a CytoFLEX S Flow Cytometer (Beckman Coulter). Typically, fluorescence
972 data for 5,000–50,000 singlet-gated cells was collected and, unless indicated otherwise, the
973 median EGFP fluorescence \pm standard error of the median (SEM = 1.253 s/n, where s = standard
974 deviation and n = sample size) was used to represent the data.

975 To measure WNT reporter activity in cells treated with the GSK3A/B inhibitor CHIR-99021,
976 ~24 hr before treatment cells were seeded in 6-well plates at a density of 0.5×10^6 per dish. Cells
977 were treated the following day with 10 μ M CHIR-99021 (CT99021) (Selleckchem Cat. # S2924)
978 or an equivalent volume of DMSO vehicle diluted in CGM 2 for 48 hr, replacing the media with
979 fresh CHIR-99021 or DMSO in CGM 2 after 24 hr of treatment. Cells were washed with 2 ml
980 PBS, harvested in 0.5 ml of 0.05% Trypsin-EDTA, resuspended in 1.5 ml of CGM 2, and EGFP
981 fluorescence was measured as described above.

982

983 **Quantitative (q)RT-PCR analysis**

984 Approximately 24 hr before treatment, cells were seeded in 24-well plates at a density of 3×10^5
985 per well and grown in 0.5 ml of CGM 2. Cells were treated for 24 hr with 50% WNT3A CM in
986 CGM 2 where indicated. The medium was removed, cells were washed once with PBS and

987 harvested in 400 μ l of TRIzol Reagent (Thermo Fisher Scientific Cat. # 15596018). Extracts
988 were processed according to the manufacturer's protocol, taking the appropriate precautions to
989 avoid contamination with nucleases, and total RNA was resuspended in 20 μ l of DEPC-treated
990 water (Thermo Fisher Scientific Cat. # AM9920). To synthesize cDNA, 125 ng of RNA were
991 diluted in 2 μ l DEPC-treated water and incubated with 0.25 μ l 10X ezDNase buffer and 0.25 μ l
992 ezDNase enzyme for 5 min at 37°C to digest DNA contaminants. After DNase treatment, 1 μ l of
993 DEPC-treated water and 1 μ l of SuperScript™ IV VILO™ MM (Invitrogen Cat. # 11766500)
994 were added and the reaction was incubated for 10 min at 25°C, 10 min at 50°C, and 5 min at
995 85°C. For each primer pair, a cDNA dilution series from a representative sample was analyzed to
996 ensure that target amplification was linear across a sufficiently broad range of cDNA
997 concentrations. cDNA was diluted 1:100 in water, and 5 μ l were mixed with 5 μ l of Power
998 SYBR Green PCR Master Mix (Applied Biosystems Cat. # 4367659) containing 400 nM each of
999 forward and reverse primer (S2 File). Triplicate reactions for each cDNA and primer pair were
1000 prepared in a MicroAmp Optical 384-well Reaction Plate (Thermo Fisher Scientific Cat. #
1001 4309849), sealed with MicroAmp Optical Adhesive Film (Thermo Fisher Scientific Cat. #
1002 4311971) and run using standard parameters in a QuantStudio 5 Real-Time PCR System
1003 (Applied Biosystems). Thermo Fisher cloud design and analysis software (DA2) was used to
1004 calculate the average relative abundance of *AXIN2*, *RNF43*, *TNFRSF19*, or *NKDI* mRNA
1005 normalized to *HPRT1* mRNA, and fold-changes in mRNA abundance were calculated as the
1006 quotient between the experimental and reference samples, with appropriate error propagation of
1007 the respective standard deviations (SD).
1008

1009 **Immunoblot analysis and quantification of soluble CTNNB1 from membrane-free**
1010 **supernatants (MFS)**

1011 Approximately 24 hr before treatment, cells were seeded in 6 cm dishes at a density of 2.5×10^6
1012 per dish and grown in 5 ml of CGM 2. Cells were treated for 24 hr with 50% WNT3A CM in
1013 CGM 2 where indicated. Cells were harvested, lysed by hypotonic shock, and extracts were
1014 prepared as follows, with all handling done at 4°C. Cells were washed twice with ~5 ml cold
1015 PBS and twice with ~5 ml cold 10 mM HEPES pH 7.4. Residual buffer was removed, and 100 μ l
1016 of ice-cold SEAT buffer (10 mM triethanolamine/acetic acid pH 7.6, 250 mM sucrose, 1X
1017 SIGMAFAST Protease Inhibitor Cocktail Tablets EDTA-free (Sigma-Aldrich Cat. # S8830), 25
1018 μ M MG132 (Sigma-Aldrich Cat. # C2211), 1X PhosSTOP (Roche Cat. # 04906837001), 1 mM
1019 NaF, 1 mM Na_3VO_4 , 1 mM dithiothreitol (DTT), 62.5 U/ml Benzonase Nuclease (EMD
1020 Millipore Cat. # 70664), 1 mM MgCl_2) were added to the cells. Cells were scraped using a cell
1021 lifter (Corning Cat. # 3008), transferred to 2-ml centrifuge tubes and disrupted mechanically by
1022 triturating 10 times. Crude extracts were centrifuged for 20 min at 20,000 x g to pellet
1023 membranes and other insoluble cellular material, and the MFS was carefully removed, avoiding
1024 contamination from the pellet. The MFS was flash-frozen in liquid nitrogen and stored at -80°C
1025 until further processing.

1026 Extracts were thawed quickly at RT and transferred to ice. The protein concentration in the
1027 MFS was quantified with the Pierce BCA Protein Assay Kit (Thermo Fisher Scientific Cat. #
1028 23225), using BSA as a standard, and samples were normalized by dilution with SEAT buffer.
1029 The MFS was diluted with 4X LDS sample buffer (Thermo Fisher Scientific Cat. # NP0007)
1030 supplemented with 50 mM tris(2-carboxyethyl)phosphine (TCEP), incubated for 45 min at RT or
1031 heated at 95°C for 10 min, and 30 μ g of total protein were electrophoresed alongside Precision

1032 Plus Protein All Blue Prestained Protein Standards (Bio-Rad Cat. # 1610373) in 4-15% TGX
1033 Stain-Free protein gels (BioRad, various Cat. numbers) at 75 V for 15 min and 100 V for 1 hr 15
1034 min using 1X Tris/Glycine/SDS running buffer (BioRad Cat. # 1610772). Following
1035 electrophoresis, the gel was briefly activated with UV light using a Chemidoc imager (BioRad)
1036 to covalently label proteins in the gel with Stain-Free fluorochromes.

1037 Proteins were transferred to PVDF membranes in a Criterion Blotter apparatus (Bio-Rad Cat.
1038 # 1704071) at 60 V for 2 hr using 1X Tris/Glycine transfer buffer (BioRad Cat. # 1610771)
1039 containing 20% methanol. Following transfer, the membrane was imaged using the ChemiDoc
1040 imager, and the total protein in each lane was quantified. Membranes were cut, blocked with
1041 Odyssey Blocking Buffer (Li-Cor Cat. # 927-40000), incubated with mouse anti- β -catenin or
1042 mouse anti-GAPDH primary antibodies, washed with TBST, incubated with IRDye 800CW
1043 donkey anti-mouse IgG secondary antibody, washed with TBST followed by TBS, and imaged
1044 using a Li-Cor Odyssey imaging system. Acquisition parameters in the manufacturer's Li-Cor
1045 Odyssey Image Studio Lite software were set so as to avoid saturated pixels in the bands of
1046 interest, and bands were quantified using background subtraction. The integrated intensity for
1047 CTNNB1 was normalized to the total protein (or in some cases to the average of total protein and
1048 the integrated intensity for GAPDH) in the corresponding lane. The average \pm SD normalized
1049 CTNNB1 intensity from duplicate blots was used to represent the data.

1050 For CHIR-99021 or DMSO vehicle treated cells, ~24 hr before treatment cells were seeded
1051 in 6 cm dishes at a density of 2×10^6 per dish and treated the following day with 10 μ M CHIR-
1052 99021 or DMSO for 48 hr. The media was replaced with fresh CHIR-99021 or DMSO in CGM 2
1053 after 24 hr of treatment.

1054

1055 **Immunoblot analyses of soluble HUWE1, APC and CSNK1A1 from MFS**

1056 Some of the same membranes used to blot for soluble CTNNB1 were cut and used to blot for
1057 other proteins as indicated in the same figures. Blots were incubated with rabbit anti-
1058 Lasu1/Ureb1 (HUWE1), mouse anti-APC and mouse anti-CSNK1A1 primary antibodies. The
1059 following secondary antibodies were used: for HUWE1, IRDye 680RD donkey anti-rabbit IgG,
1060 for APC, IRDye 800CW donkey anti-mouse IgG (both were imaged using a Li-Cor Odyssey
1061 imaging system) and for CSNK1A1, peroxidase AffiniPure goat anti-mouse IgG (developed
1062 using SuperSignal West Femto Maximum Sensitivity Substrate (Thermo Fisher Scientific Cat. #
1063 34095)).

1064

1065 **Immunoblot analysis of total HUWE1, APC, CTNNB1, AXIN1, AXIN2, GSK3A/B and**
1066 **CSNK1A1 from whole cell extracts (WCE)**

1067 Approximately 72 hr before harvest, cells were seeded in 10 cm dishes at a density of 3×10^6 per
1068 dish and grown in 10 ml of CGM 2. Cells were harvested in 2 ml Trypsin-EDTA (0.05%) and
1069 resuspended in 6 ml CGM 2. 10×10^6 cells were centrifuged at $400 \times g$ for 5 min, washed in 5 ml
1070 PBS, and centrifuged at $400 \times g$ for 5 min. The supernatant was aspirated, and the cell pellets
1071 were flash-frozen in liquid nitrogen and stored at -80°C . Pellets were thawed quickly at RT and
1072 transferred to ice. All subsequent steps were done on ice. The cell pellets were resuspended in
1073 150 μl of ice-cold RIPA lysis buffer (50 mM Tris-HCl pH 8.0, 150 mM NaCl, 2% NP-40, 0.25%
1074 deoxycholate, 0.1% SDS, 1X SIGMAFAST protease inhibitors, 1 mM MgCl_2 , 62.5 U/ml
1075 Benzonase Nuclease, 1 mM DTT, 10% glycerol), sonicated in a Bioruptor Pico sonication device
1076 (Diagenode) 4 x 30 s in the ultra-high setting, centrifuged 10 min at $20,000 \times g$ and the
1077 supernatant (WCE) was recovered.

1078 The protein concentration in the WCE was quantified using the Pierce BCA Protein Assay
1079 Kit. Samples were normalized by dilution with RIPA lysis buffer, further diluted with 4X LDS
1080 sample buffer supplemented with 50 mM TCEP, incubated for 45 min at RT, and 30 µg of total
1081 protein were electrophoresed alongside Precision Plus Protein All Blue Prestained Protein
1082 Standards in 4-15% Criterion TGX Stain-Free protein gels at 75 V for 15min, and 100 V for 1 hr
1083 and 15 min using 1X Tris/Glycine/SDS running buffer.

1084 Proteins were transferred at 60 V for 2 hr to PVDF membranes using 1X Tris/Glycine
1085 transfer buffer containing 20% methanol, and membranes were cut and blocked with either
1086 Odyssey Intercept Blocking Buffer or TBST, 5% skim milk. Blots were incubated with rabbit
1087 anti-Las1/Ureb1 (HUWE1), rabbit anti-APC, mouse anti-β-catenin, rabbit anti-AXIN1, rabbit
1088 anti-AXIN2, rabbit anti-GSK3A/B, mouse anti-CSNK1A1 and mouse anti-GAPDH (as a loading
1089 control) primary antibodies, washed with TBST, incubated with Peroxidase AffiniPure anti-
1090 rabbit or anti-mouse secondary antibodies, washed with TBST followed by TBS, and developed
1091 with SuperSignal West Femto.

1092

1093 **Immunoblot analysis and quantification of non-phospho-CTNNB1 (S33/S37/T41) and total**
1094 **CTNNB1 from WCE**

1095 Approximately 24 hr before treatment, cells were seeded in 6 cm dishes at a density of 2 x
1096 10⁶ per dish and treated the following day with 10 µM CHIR-99021 or an equivalent volume of
1097 DMSO vehicle for 48 hr. The media was replaced with fresh CHIR-99021 or DMSO in CGM 2
1098 after 24 hr of treatment. Cells were harvested in 1 ml Trypsin-EDTA (0.05%) and resuspended in
1099 3 ml CGM 2. Cells were centrifuged at 400 x g for 5 min, washed in 5 ml PBS, and centrifuged
1100 at 400 x g for 5 min. The above protocol for immunoblot analysis of total proteins from WCE

1101 was followed, except that protein samples were heated at 95°C for 10 min prior to
1102 electrophoresis, and the total protein in each lane was quantified as follows and used for
1103 normalization. Following electrophoresis, the gel was briefly activated with UV light using a
1104 Chemidoc imager (BioRad) to covalently label proteins in the gel with Stain-Free fluorochromes.
1105 Following transfer, the membrane was imaged using the ChemiDoc, and the total protein in each
1106 lane was quantified. The blots were incubated with rabbit non-phospho (active) β -catenin (Ser33-
1107 37-Thr41), mouse anti- β -catenin or mouse anti-GAPDH (as a loading control) primary
1108 antibodies, IRDye 680RD donkey anti-rabbit IgG or IRDye 800CW donkey anti-mouse IgG
1109 secondary antibodies, and imaged using a Li-Cor Odyssey imaging system.

1110

1111 **Quantitative dot blot of HUWE1 from WCE**

1112 3 μ l WCE containing 8 μ g protein were spotted onto nitrocellulose membrane for each sample in
1113 triplicate. The membrane was allowed to dry for 15 min prior to staining with Revert 520 Total
1114 Protein Stain (Li-Cor Cat. # 926-10010) according to the manufacturer's protocol
1115 (<https://www.licor.com/documents/1o8anlg26tnwqkj135ki6bo61fy4ztmi>). The membrane was
1116 imaged on the Li-Cor Odyssey M imaging system using the 520 nm channel to obtain a total
1117 protein quantification for normalization. The membrane was then blocked with Odyssey
1118 Blocking Buffer, incubated with rabbit anti-Lasul/Ureb1 (HUWE1), washed with TBST,
1119 incubated with IRDye 680RD donkey anti-rabbit IgG secondary antibody, washed with TBST
1120 followed by TBS, and imaged using the Li-Cor Odyssey M imaging system. Acquisition
1121 parameters in the manufacturer's Li-Cor Odyssey Image Studio Lite software were set so as to
1122 avoid saturated pixels in the dots of interest, and dots were quantified using background
1123 subtraction. The integrated intensity for HUWE1 was normalized to that for Revert 520 Total

1124 Protein Stain in the same blot, and the average \pm SD from triplicate dot blots was used to
1125 represent the data. The specificity of the HUWE1 signal was confirmed by comparing dot blots
1126 of WCE from CSNK1A1^{KO} and CSNK1A1^{KO}; HUWE1^{KO} cells. All normalized HUWE1
1127 intensity values were within the linear range of a standard curve prepared from dot blots of a
1128 serial dilution of WCE from CSNK1A1^{KO} cells.

1129

1130 **Preparation of figures and statistical analysis**

1131 Figures were prepared using PowerPoint (Microsoft). Table 1, S1 and S2 Files were prepared
1132 using Excel (Microsoft). Graphs were prepared and statistical analysis performed using Prism 6
1133 (GraphPad) or Excel. Details of the statistical tests used are given in the figure legends.

1134 Significance is indicated as ****(p<0.0001), *** (p<0.001), ** (p<0.01), * (p<0.05) or n.s. (not
1135 significant). Pictures of immunoblots were adjusted for contrast and brightness only when
1136 necessary for clarity using Image Studio Lite (LiCor), and were arranged in PowerPoint.

1137

1138 **Acknowledgments:**

1139

1140 AML was supported by the Intramural Research Program of the National Institutes of Health,

1141 National Cancer Institute, Center for Cancer Research. We thank Caleb K. Sinclear for help with

1142 experiments, Lebensohn Lab members and members of the Laboratory of Cellular and Molecular

1143 Biology for input on the project, Rajat Rohatgi for feedback on the manuscript, and the Center

1144 for Cancer Research Genomics Core and the Laboratory of Genome Integrity Flow Cytometry

1145 Core for assistance and services. The authors declare no conflicting financial interests.

1146

1147 **References:**

1148

- 1149 1. Nusse R, He X, Amerongen Rv. Wnt signaling : a subject collection from Cold Spring
1150 Harbor Perspectives in Biology. Cold Spring Harbor, N.Y.: Cold Spring Harbor Laboratory
1151 Press; 2013. vii, 454 p. p.
- 1152 2. Hoppler S, Moon RT. Wnt signaling in development and disease : molecular mechanisms
1153 and biological functions. Hoboken, New Jersey: Wiley Blackwell; 2014. ix, 459 pages p.
- 1154 3. Nusse R, Clevers H. Wnt/beta-Catenin Signaling, Disease, and Emerging Therapeutic
1155 Modalities. Cell. 2017;169(6):985-99.
- 1156 4. Anastas JN, Moon RT. WNT signalling pathways as therapeutic targets in cancer. Nat
1157 Rev Cancer. 2013;13(1):11-26.
- 1158 5. Stamos JL, Weis WI. The beta-catenin destruction complex. Cold Spring Harb Perspect
1159 Biol. 2013;5(1):a007898.
- 1160 6. Liu C, Li Y, Semenov M, Han C, Baeg GH, Tan Y, et al. Control of beta-catenin
1161 phosphorylation/degradation by a dual-kinase mechanism. Cell. 2002;108(6):837-47.
- 1162 7. Amit S, Hatzubai A, Birman Y, Andersen JS, Ben-Shushan E, Mann M, et al. Axin-
1163 mediated CKI phosphorylation of beta-catenin at Ser 45: a molecular switch for the Wnt
1164 pathway. Genes Dev. 2002;16(9):1066-76.
- 1165 8. Yost C, Torres M, Miller JR, Huang E, Kimelman D, Moon RT. The axis-inducing
1166 activity, stability, and subcellular distribution of beta-catenin is regulated in Xenopus embryos
1167 by glycogen synthase kinase 3. Genes Dev. 1996;10(12):1443-54.
- 1168 9. Orford K, Crockett C, Jensen JP, Weissman AM, Byers SW. Serine phosphorylation-
1169 regulated ubiquitination and degradation of beta-catenin. J Biol Chem. 1997;272(40):24735-8.

- 1170 10. Wu G, Xu G, Schulman BA, Jeffrey PD, Harper JW, Pavletich NP. Structure of a beta-
1171 TrCP1-Skp1-beta-catenin complex: destruction motif binding and lysine specificity of the
1172 SCF(beta-TrCP1) ubiquitin ligase. *Mol Cell*. 2003;11(6):1445-56.
- 1173 11. Gammons M, Bienz M. Multiprotein complexes governing Wnt signal transduction. *Curr*
1174 *Opin Cell Biol*. 2018;51:42-9.
- 1175 12. Colozza G, Koo BK. Wnt/beta-catenin signaling: Structure, assembly and endocytosis of
1176 the signalosome. *Dev Growth Differ*. 2021;63(3):199-218.
- 1177 13. Anthony CC, Robbins DJ, Ahmed Y, Lee E. Nuclear Regulation of Wnt/beta-Catenin
1178 Signaling: It's a Complex Situation. *Genes (Basel)*. 2020;11(8).
- 1179 14. Wiese KE, Nusse R, van Amerongen R. Wnt signalling: conquering complexity.
1180 *Development*. 2018;145(12).
- 1181 15. Lebensohn AM, Dubey R, Neitzel LR, Tacchelly-Benites O, Yang E, Marceau CD, et al.
1182 Comparative genetic screens in human cells reveal new regulatory mechanisms in WNT
1183 signaling. *Elife*. 2016;5.
- 1184 16. Carette JE, Guimaraes CP, Wuethrich I, Blomen VA, Varadarajan M, Sun C, et al.
1185 Global gene disruption in human cells to assign genes to phenotypes by deep sequencing. *Nat*
1186 *Biotechnol*. 2011;29(6):542-6.
- 1187 17. Giles AC, Grill B. Roles of the HUWE1 ubiquitin ligase in nervous system development,
1188 function and disease. *Neural Dev*. 2020;15(1):6.
- 1189 18. Gong X, Du D, Deng Y, Zhou Y, Sun L, Yuan S. The structure and regulation of the E3
1190 ubiquitin ligase HUWE1 and its biological functions in cancer. *Invest New Drugs*.
1191 2020;38(2):515-24.

- 1192 19. Kao SH, Wu HT, Wu KJ. Ubiquitination by HUWE1 in tumorigenesis and beyond. J
1193 Biomed Sci. 2018;25(1):67.
- 1194 20. Qi L, Xu X, Qi X. The giant E3 ligase HUWE1 is linked to tumorigenesis,
1195 spermatogenesis, intellectual disability, and inflammatory diseases. Front Cell Infect Microbiol.
1196 2022;12:905906.
- 1197 21. Staal FJ, van Noort M, Strous GJ, Clevers HC. Wnt signals are transmitted through N-
1198 terminally dephosphorylated beta-catenin. EMBO Rep. 2002;3(1):63-8.
- 1199 22. Aberle H, Bauer A, Stappert J, Kispert A, Kemler R. beta-catenin is a target for the
1200 ubiquitin-proteasome pathway. EMBO J. 1997;16(13):3797-804.
- 1201 23. Boonekamp KE, Heo I, Artegiani B, Asra P, van Son G, de Ligt J, Clevers H.
1202 Identification of novel human Wnt target genes using adult endodermal tissue-derived organoids.
1203 Dev Biol. 2021;474:37-47.
- 1204 24. Yan D, Wallingford JB, Sun TQ, Nelson AM, Sakanaka C, Reinhard C, et al. Cell
1205 autonomous regulation of multiple Dishevelled-dependent pathways by mammalian Nkd. Proc
1206 Natl Acad Sci U S A. 2001;98(7):3802-7.
- 1207 25. Schon S, Flierman I, Ofner A, Stahringer A, Holdt LM, Kolligs FT, Herbst A. beta-
1208 catenin regulates NF-kappaB activity via TNFRSF19 in colorectal cancer cells. Int J Cancer.
1209 2014;135(8):1800-11.
- 1210 26. Qi LS, Larson MH, Gilbert LA, Doudna JA, Weissman JS, Arkin AP, Lim WA.
1211 Repurposing CRISPR as an RNA-guided platform for sequence-specific control of gene
1212 expression. Cell. 2013;152(5):1173-83.

- 1213 27. Hunkeler M, Jin CY, Ma MW, Monda JK, Overwijn D, Bennett EJ, Fischer ES. Solenoid
1214 architecture of HUWE1 contributes to ligase activity and substrate recognition. *Mol Cell*.
1215 2021;81(17):3468-80 e7.
- 1216 28. Bernassola F, Karin M, Ciechanover A, Melino G. The HECT family of E3 ubiquitin
1217 ligases: multiple players in cancer development. *Cancer Cell*. 2008;14(1):10-21.
- 1218 29. Koblan LW, Doman JL, Wilson C, Levy JM, Tay T, Newby GA, et al. Improving
1219 cytidine and adenine base editors by expression optimization and ancestral reconstruction. *Nat*
1220 *Biotechnol*. 2018;36(9):843-6.
- 1221 30. Moshkovsky AR, Ma W, Kirschner MW. The self-regulated response of the Wnt
1222 pathway to an oncogenic mutation in β -catenin. *bioRxiv*. 2021:2021.05.05.442673.
- 1223 31. Wang Z, Vogelstein B, Kinzler KW. Phosphorylation of beta-catenin at S33, S37, or T41
1224 can occur in the absence of phosphorylation at T45 in colon cancer cells. *Cancer Res*.
1225 2003;63(17):5234-5.
- 1226 32. Chia IV, Costantini F. Mouse axin and axin2/conductin proteins are functionally
1227 equivalent in vivo. *Mol Cell Biol*. 2005;25(11):4371-6.
- 1228 33. de Groot RE, Ganji RS, Bernatik O, Lloyd-Lewis B, Seipel K, Sedova K, et al. Huwe1-
1229 mediated ubiquitylation of dishevelled defines a negative feedback loop in the Wnt signaling
1230 pathway. *Sci Signal*. 2014;7(317):ra26.
- 1231 34. Dominguez-Brauer C, Khatun R, Elia AJ, Thu KL, Ramachandran P, Baniasadi SP, et al.
1232 E3 ubiquitin ligase Mule targets beta-catenin under conditions of hyperactive Wnt signaling.
1233 *Proc Natl Acad Sci U S A*. 2017;114(7):E1148-E57.

- 1234 35. Vandewalle J, Langen M, Zschatzsch M, Nijhof B, Kramer JM, Brems H, et al. Ubiquitin
1235 ligase HUWE1 regulates axon branching through the Wnt/beta-catenin pathway in a *Drosophila*
1236 model for intellectual disability. *PLoS One*. 2013;8(11):e81791.
- 1237 36. Dominguez-Brauer C, Hao Z, Elia AJ, Fortin JM, Nechanitzky R, Brauer PM, et al. Mule
1238 Regulates the Intestinal Stem Cell Niche via the Wnt Pathway and Targets EphB3 for
1239 Proteasomal and Lysosomal Degradation. *Cell Stem Cell*. 2016;19(2):205-16.
- 1240 37. Fiedler M, Mendoza-Topaz C, Rutherford TJ, Mieszczanek J, Bienz M. Dishevelled
1241 interacts with the DIX domain polymerization interface of Axin to interfere with its function in
1242 down-regulating beta-catenin. *Proc Natl Acad Sci U S A*. 2011;108(5):1937-42.
- 1243 38. Schwarz-Romond T, Fiedler M, Shibata N, Butler PJ, Kikuchi A, Higuchi Y, Bienz M.
1244 The DIX domain of Dishevelled confers Wnt signaling by dynamic polymerization. *Nat Struct*
1245 *Mol Biol*. 2007;14(6):484-92.
- 1246 39. Su C, Wang T, Zhao J, Cheng J, Hou J. Meta-analysis of gene expression alterations and
1247 clinical significance of the HECT domain-containing ubiquitin ligase HUWE1 in cancer. *Oncol*
1248 *Lett*. 2019;18(3):2292-303.
- 1249 40. Wang JY, Doudna JA. CRISPR technology: A decade of genome editing is only the
1250 beginning. *Science*. 2023;379(6629):eadd8643.
- 1251 41. Horii T, Hatada I. Genome Editing Using Mammalian Haploid Cells. *Int J Mol Sci*.
1252 2015;16(10):23604-14.
- 1253 42. Li Y, Shuai L. A versatile genetic tool: haploid cells. *Stem Cell Res Ther*. 2017;8(1):197.
- 1254 43. Dubey R, van Kerkhof P, Jordens I, Malinauskas T, Pusapati GV, McKenna JK, et al. R-
1255 spondins engage heparan sulfate proteoglycans to potentiate WNT signaling. *Elife*. 2020;9.

- 1256 44. Shalem O, Sanjana NE, Hartenian E, Shi X, Scott DA, Mikkelsen T, et al. Genome-scale
1257 CRISPR-Cas9 knockout screening in human cells. *Science*. 2014;343(6166):84-7.
- 1258 45. Doench JG, Hartenian E, Graham DB, Tothova Z, Hegde M, Smith I, et al. Rational
1259 design of highly active sgRNAs for CRISPR-Cas9-mediated gene inactivation. *Nat Biotechnol*.
1260 2014;32(12):1262-7.
- 1261 46. Hsu PD, Scott DA, Weinstein JA, Ran FA, Konermann S, Agarwala V, et al. DNA
1262 targeting specificity of RNA-guided Cas9 nucleases. *Nat Biotechnol*. 2013;31(9):827-32.
- 1263 47. Cong L, Ran FA, Cox D, Lin S, Barretto R, Habib N, et al. Multiplex genome
1264 engineering using CRISPR/Cas systems. *Science*. 2013;339(6121):819-23.
- 1265 48. Arbab M, Shen MW, Mok B, Wilson C, Matuszek Z, Cassa CA, Liu DR. Determinants
1266 of Base Editing Outcomes from Target Library Analysis and Machine Learning. *Cell*.
1267 2020;182(2):463-80 e30.
- 1268 49. Chari R, Yeo NC, Chavez A, Church GM. sgRNA Scorer 2.0: A Species-Independent
1269 Model To Predict CRISPR/Cas9 Activity. *ACS Synth Biol*. 2017;6(5):902-4.
- 1270 50. Gooden AA, Evans CN, Sheets TP, Clapp ME, Chari R. dbGuide: a database of
1271 functionally validated guide RNAs for genome editing in human and mouse cells. *Nucleic Acids*
1272 *Res*. 2021;49(D1):D871-D6.
- 1273

1274 **Figure legends:**

1275

1276 **Fig 1. HUWE1 and AXIN1 reciprocally regulate WNT signaling by modulating**

1277 **GSK3A/GSK3B-dependent CTNNB1 phosphorylation and abundance.**

1278 (A-C). We note that the data for WT HAP-7TGP, CSNK1A1^{KO} and CSNK1A1^{KO}; HUWE1^{KO}
1279 cells is discussed in the first section of the results, while the data for CSNK1A1^{KO}; AXIN1^{OE} and
1280 CSNK1A1^{KO}; HUWE1^{KO}; AXIN1^{OE} cells is discussed in a later section of the results subtitled
1281 “HUWE1 enhances WNT signaling by antagonizing the DC.” Cells were treated with DMSO
1282 vehicle or 10 μ M of the GSK3A/GSK3B inhibitor CHIR-99021 for 48 hr as indicated. (A) WNT
1283 reporter activity (median EGFP fluorescence from 10,000 singlets was measured for triplicate
1284 wells and the average \pm standard deviation (SD) of the three measurements is depicted), relative
1285 to WT HAP1-7TGP cells treated with DMSO. Significance was determined by unpaired t-test
1286 with Welch’s correction. (B) Soluble CTNNB1 abundance (CTNNB1 intensity normalized to
1287 total protein, average \pm SD from duplicate immunoblots shown in S1A Fig) in membrane-free
1288 supernatants (MFS) of the indicated cell lines, relative to WT HAP1-7TGP cells treated with
1289 DMSO. (C) Non-phospho-CTNNB1 (S33/S37/T41) abundance (non-phospho-CTNNB1
1290 intensity normalized to total protein, average \pm SD from duplicate immunoblots shown in S1B
1291 Fig) in whole cell extracts (WCE) of the indicated cell lines, relative to WT HAP1-7TGP cells
1292 treated with DMSO.

1293

1294 **S1 Fig. HUWE1 and AXIN1 reciprocally regulate WNT signaling by modulating**

1295 **GSK3A/GSK3B-dependent CTNNB1 phosphorylation and abundance.**

1296 (A-C) We note that the data for WT HAP1-7TGP, CSNK1A1^{KO} and CSNK1A1^{KO}; HUWE1^{KO}
1297 cells is discussed in the first section of the results, while the data for CSNK1A1^{KO}; AXIN1^{OE} and
1298 CSNK1A1^{KO}; HUWE1^{KO}; AXIN1^{OE} cells is discussed in a later section of the results subtitled
1299 “HUWE1 enhances WNT signaling by antagonizing the DC.” Cells were treated with DMSO
1300 vehicle or 10 μ M of the GSK3A/GSK3B inhibitor CHIR-99021 for 48 hr as indicated. (A)
1301 Immunoblots of soluble CTNNB1 from MFS, used for quantification in Fig 1B. (B)
1302 Immunoblots of non-phospho-CTNNB1 (S33/S37/T41) and total CTNNB1 from WCE, used for
1303 quantification in Fig 1C and S1C Fig, respectively. (C) Total CTNNB1 abundance (CTNNB1
1304 intensity normalized to total protein, average \pm SD from duplicate immunoblots shown in S1B)
1305 in WCE of the indicated cell lines, relative to WT HAP1-7TGP cells treated with DMSO. (D)
1306 Immunoblot analysis of total AXIN1 from WCE of the indicated cell lines used in A-C, and in
1307 Fig 1. The polyclonal cell populations overexpressing AXIN1 were generated as described in
1308 Materials and methods. AXIN1 abundance (AXIN1 intensity normalized to GAPDH intensity),
1309 relative to CSNK1A1^{KO} cells, is indicated below the blots.

1310

1311 **Fig 2. HUWE1 enhances WNT signaling through a mechanism independent of CTNNB1**
1312 **stability.**

1313 (A-F) Each circle represents a unique clonal cell line (determined by genotyping, S1 File). The
1314 same cell lines were used in A-F. A single value for the parental WT HAP1-7TGP cell line, and
1315 the average value from 3 independent clonal cell lines for each of the other genotypes, all
1316 relative to the untreated WT HAP1-7TGP sample, are indicated by a horizontal line and
1317 quantified above each group of circles. WT HAP1-7TGP cells were treated with 50% WNT3A
1318 CM for 24 hr where indicated. Significance was determined by unpaired t-test with Welch’s

1319 correction. (A) Relative soluble CTNNB1 abundance (CTNNB1 intensity normalized to total
1320 protein and GAPDH intensity, average from duplicate immunoblots shown in S2B Fig) in MFS
1321 of the indicated cell lines. (B) Relative WNT reporter activity (median EGFP fluorescence from
1322 100,000 singlets). (C-F) Relative WNT target gene expression (average quantification of *AXIN2*,
1323 *RNF43*, *TNFRSF19*, or *NKDI* mRNA normalized to *HPRT1* mRNA, each measured in triplicate
1324 reactions).

1325

1326 **S2 Fig. HUWE1 enhances WNT signaling through a mechanism independent of CTNNB1**
1327 **stability.**

1328 (A) Genomic nucleotide and corresponding amino acid sequences comprising the CTNNB1
1329 phosphodegron of WT HAP1-7TGP and CTNNB1^{ST-A} cells. The kinases that phosphorylate S or
1330 T residues in the phosphodegron are indicated. Nucleotides and amino acids in red indicate
1331 mutations. (B) Immunoblots of soluble HUWE1 and CTNNB1 from MFS of the indicated cell
1332 lines. The CTNNB1 immunoblots were used for quantification in Fig 2A. (C-E) Treatment of
1333 CTNNB1^{ST-A} cells with WNT3A does not promote further accumulation of soluble CTNNB1
1334 and does not further increase WNT target gene expression. Cells were treated with 50% WNT3A
1335 CM for 24 hr where indicated. (C) Immunoblots of total CTNNB1 from WCE used for
1336 quantification in D. (D) Total CTNNB1 abundance (CTNNB1 intensity normalized to total
1337 protein and GAPDH intensity, average \pm SD from duplicate lanes of the immunoblots shown in
1338 C) in WCE of CTNNB1^{ST-A} cells treated with WNT3A CM, relative to untreated CTNNB1^{ST-A}
1339 cells. Significance was determined by unpaired t-test with Welch's correction. (E) mRNA
1340 abundance (average \pm SD *AXIN2*, *RNF43*, *TNFRSF19*, or *NKDI* mRNA normalized to *HPRT1*
1341 mRNA, each measured in triplicate reactions) in CTNNB1^{ST-A} cells treated with WNT3A CM,

1342 reported as percentage of the mRNA abundance in untreated CTNNB1^{ST-A} cells. (F) WNT
1343 reporter activity (median EGFP fluorescence from 5,000 singlets) for the indicated cell lines,
1344 relative to the average for CTNNB1^{ST-A} cells. Each circle represents a unique clonal cell line
1345 (determined by genotyping, S1 File), and the average of 9-12 independent clones for each
1346 genotype is indicated by a horizontal line and quantified above each group of circles.
1347 Significance was determined by unpaired t-test with Welch's correction.

1348

1349 **Fig 3. HUWE1 enhances WNT signaling through mechanisms mediated by APC.**

1350 (A-F) The same cell lines were used in A-F. WT cells were treated with 50% WNT3A CM for
1351 24 hr where indicated. (A) Immunoblot analysis of soluble proteins from MFS of the indicated
1352 clonal cell lines. We note that CSNK1A1^{KO-2} cells contain a loss-of-function mutation resulting
1353 in a 2-amino acid deletion (S1 File), and hence the protein product is still present. The “a” and
1354 “b” superscripts next to the protein names indicate which of two membranes the corresponding
1355 strips were cut from. * indicates a non-specific band observed with the mouse anti-APC
1356 antibody. (B-F) Each circle represents a unique clonal cell line (determined by genotyping, S1
1357 File). A single value for the parental WT HAP1-7TGP cell line, and the average value from 2-3
1358 independent clonal cell lines for each of the other genotypes, all relative to the untreated WT
1359 HAP1-7TGP sample, are indicated by a horizontal line and quantified above each group of
1360 circles. Significance was determined by unpaired t-test with Welch's correction. (B) Relative
1361 soluble CTNNB1 abundance (CTNNB1 intensity normalized to total protein, average from
1362 duplicate immunoblots) in MFS of the indicated cell lines. (C-F) Relative WNT target gene
1363 expression (average quantification of *AXIN2*, *RNF43*, *TNFRSF19*, or *NKDI* mRNA normalized
1364 to *HPRT1* mRNA, each measured in triplicate reactions).

1365

1366 **Fig 4. HUWE1 enhances WNT signaling through mechanisms mediated by a subset of DC**
1367 **components including APC, AXIN1 and GSK3A or GSK3B.**

1368 (A-E) The same cell lines are used in A-E. WT HAP1-7TGP cells were treated with 50%
1369 WNT3A CM for 24 hr where indicated. (A) Aggregate WNT target gene expression (average \pm
1370 SD of all four target genes, calculated from the individual average quantifications of *AXIN2*,
1371 *RNF43*, *TNFRSF19* or *NKDI* mRNA normalized to *HPRT1* mRNA, each measured in triplicate
1372 reactions) in polyclonal cell populations targeted with HUWE1 sgRNAs, reported as percentage
1373 of aggregate WNT target gene expression in polyclonal cell populations targeted with SCR
1374 sgRNA control. Significance was determined by unpaired t-test with Welch's correction. (B-E)
1375 WNT target gene expression (average \pm SD *AXIN2*, *RNF43*, *TNFRSF19*, or *NKDI* mRNA
1376 normalized to *HPRT1* mRNA, each measured in triplicate reactions) in polyclonal cell
1377 populations targeted with HUWE1 sgRNAs, reported as percentage of WNT target gene
1378 expression in polyclonal cell populations targeted with SCR sgRNA control.

1379

1380 **S4 Fig. HUWE1 enhances WNT signaling through mechanisms mediated by a subset of DC**
1381 **components including APC, AXIN1 and GSK3A or GSK3B.**

1382 (A) Immunoblot analysis of total protein from WCE of the indicated clonal cell lines used for
1383 CRISPRi-mediated HUWE1 KD in Fig 4 and S5 Fig. The AXIN1 and AXIN2 immunoblots of
1384 *CSNK1A1^{KO}*; *AXIN1^{KO}* and *CSNK1A1^{KO}*; *AXIN2^{KO}* cells, respectively, exhibited bands of
1385 lower abundance and molecular weight than their respective counterparts in WT HAP1-7TGP
1386 cells. These bands may represent residual truncated protein products, but in both cases frameshift
1387 mutations in the single allele of the respective genes (S1 File) predicted the absence of full-

1388 length, WT proteins. * indicates a non-specific band observed with the rabbit anti-APC antibody.
1389 The “a” and “b” superscripts next to the protein names indicate which of two membranes the
1390 corresponding strips were cut from. Dashed vertical lines indicate a rearrangement of samples
1391 within the same blot. (B, C) GSK3A and GSK3B are functionally redundant in WNT signaling
1392 in HAP1 cells. The same cell lines were used in B and C. (B) Immunoblot analysis of total
1393 GSK3A and GSK3B from WCE of the indicated cell lines. (C) WNT reporter activity (median
1394 EGFP fluorescence from 50,000 singlets was measured for biological duplicates of a single
1395 clone, and the average \pm SD of the two measurements was calculated) relative to untreated WT
1396 HAP1-7TGP cells. (D) HUWE1 abundance, quantified by dot blots, in the clonal cell lines used
1397 for CRISPRi-mediated HUWE1 KD in Fig 4 and S5 Fig. Total HUWE1 abundance (HUWE1
1398 intensity normalized to total protein, average \pm SD from triplicate dot blots) in WCE of the
1399 indicated cell lines, relative to WT HAP1-7TGP cells. Significance was determined by unpaired
1400 t-test with Welch’s correction, and the difference in HUWE1 abundance between each mutant
1401 cell line and WT HAP1-7TGP cells was not significant (not depicted).

1402

1403 **S5 Fig. Quantification of CRISPRi-mediated HUWE1 KD in various genetic backgrounds.**

1404 (A-B) Two polyclonal cell populations targeted with HUWE1 sgRNAs (1 and 2) and one
1405 polyclonal cell population targeted with SCR sgRNA were derived for each genotype as
1406 described in Materials and methods. (A) Immunoblots of total HUWE1 from WCE used for
1407 quantification in B. The “a” and “b” superscripts next to the protein names indicate which of two
1408 duplicate membranes the corresponding strips were cut from. Dashed vertical lines indicate a
1409 rearrangement of samples within the same blot. (B) HUWE1 abundance (average HUWE1
1410 intensity normalized to either Na⁺/K⁺ ATPase or GAPDH intensity from duplicate immunoblots

1411 shown in A) in WCE of cell populations targeted with HUWE1 sgRNAs, reported as percentage
1412 of HUWE1 abundance in WCE of cell populations targeted with SCR sgRNA control.

1413

1414 **Fig 5. Regulation of WNT signaling by HUWE1 requires its ubiquitin ligase activity.**

1415 (A) WNT reporter activity (median \pm standard error of the median (SEM) EGFP fluorescence
1416 from 37,000-50,000 cells) of one CSNK1A1^{KO}; HUWE1^{KO} clonal cell line and three catalytic
1417 mutant CSNK1A1^{KO}; HUWE1^{C4341R} clonal cell lines, relative to CSNK1A1^{KO} cells. (B-D) WNT
1418 target gene expression (average \pm SD *AXIN2*, *RNF43* or *TNFSRF19* mRNA normalized to
1419 *HPRT1* mRNA, each measured in triplicate reactions) of the indicated clonal cell lines, relative
1420 to CSNK1A1^{KO} cells. (E) Immunoblot analysis of total HUWE1 protein in WCE of the same cell
1421 lines used in A-D.

1422

1423 **S6 Fig. Quantification of CRISPR/Cas9-mediated *HUWE1* mutations in HEK293T-7TG
1424 and HEK293T-7TG CSNK1A1^{KO} cells.**

1425 (A, B) Sequencing reads of the *HUWE1* locus targeted by CRISPR/Cas9 in individual clonal cell
1426 lines derived from HEK293T-7TG (A) or HEK293T-7TG CSNK1A1^{KO} (B) cells were quantified
1427 for mutations. The X-axis shows individual clones, and the Y-axis indicates the percentage of
1428 reads containing mutations. Bars in dark blue indicate the percentage of reads containing any
1429 kind of mutation (total mutations) at the targeted locus in each clone, and bars in light blue
1430 indicate the percentage of reads containing out-of-frame mutations at the same locus. In all 113
1431 clones in which ~100% of the reads contained mutations (indicating all *HUWE1* alleles had been
1432 successfully targeted), some of those mutations were always in frame, strongly suggesting that at
1433 least one WT *HUWE1* allele is required for cell viability in HEK293T cells.

1434

1435 **Supporting Information:**

1436

1437 **S1 File. CRISPR/Cas9-engineered clonal cell lines used in this study.**

1438 Single-mutant clones in which a single gene was targeted using CRISPR/Cas9 and double- or
1439 triple-mutant clones in which multiple genes were targeted using CRISPR/Cas9 are described in
1440 two separate spreadsheets labeled accordingly. When more than one clone was generated using
1441 the same CRISPR guide, the ‘Clone Name’ column indicates the generic name used throughout
1442 the manuscript to describe the genotype, and the ‘Clone #’ column identifies an individual clone.
1443 The ‘HDR Donor’ column indicates the name of the ssODN donor template used to generate
1444 some of the clonal cell lines (see Materials and Methods). The ‘CRISPR guide’ column indicates
1445 the name of the guide used, which is the same as that of the oligos encoding sgRNAs (see
1446 Materials and methods, and S2 File). The ‘Genomic Sequence’ column shows 80 bases of
1447 genomic sequence (5’ relative to the gene is to the left) surrounding the target site. For each
1448 group of clones made using the same CRISPR guide (separated by gray spacers), the ‘Genomic
1449 Sequence’ column is headlined by the reference WT genomic sequence (obtained from RefSeq),
1450 with the guide sequence colored blue. The site of the double strand cut made by Cas9 is between
1451 the two underlined bases. Sequencing results for individual clones are indicated below the
1452 reference sequence. Some clones that remained WT at the targeted locus are indicated as such
1453 and were used as controls. For mutant clones, mutated bases are colored red (dashes represent
1454 deleted bases, three dots are used to indicate that a deletion continues beyond the 80 bases of
1455 sequence shown, and large insertions are indicated in brackets), and the nature of the mutation
1456 and the resulting genotype are described in the columns labeled accordingly. The figures in
1457 which each clone was used are also indicated. For double- and triple-mutant clones, the CRISPR

1458 guide used, the genomic sequence, the mutation and the genotype pertaining to each of the two
1459 or three targeted loci are designated ‘1’, ‘2’ and ‘3’ in the column headings, and are shown under
1460 green, orange and purple spacers, respectively.

1461

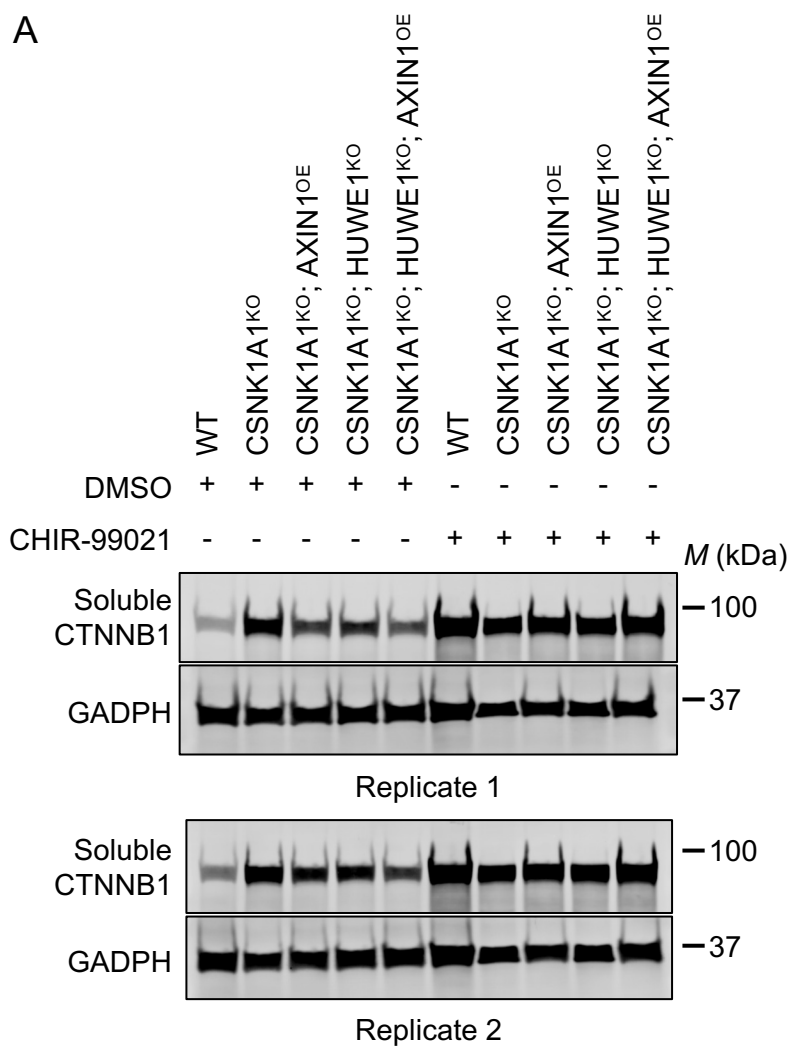
1462 **S2 File. Oligonucleotides and primers used in this study.**

1463 Oligonucleotides and primers used for generation and characterization of clonal cell lines
1464 engineered using CRISPR/Cas9 nuclease (CRISPRn), base editing, and CRISPRi, as well as
1465 those used for qRT-PCR, are described in separate spreadsheets labeled accordingly. CRISPRn,
1466 base editing and CRISPRi: the names and sequences of pairs of oligonucleotides encoding
1467 sgRNAs, which were cloned into the respective vectors for each application as described in
1468 Materials and methods, are shown in columns A and B, respectively. Additionally, for CRISPRn
1469 and base editing the names and sequences of pairs of forward and reverse primers used to
1470 amplify corresponding genomic regions flanking sgRNA target sites are shown in columns C and
1471 D, respectively, and where applicable, the names and sequences of individual primers used to
1472 sequence the amplified target sites are shown in columns E and F, respectively. qRT-PCR: the
1473 names and sequences of pairs of forward and reverse primers used for qRT-PCR are shown in
1474 columns A and B, respectively.

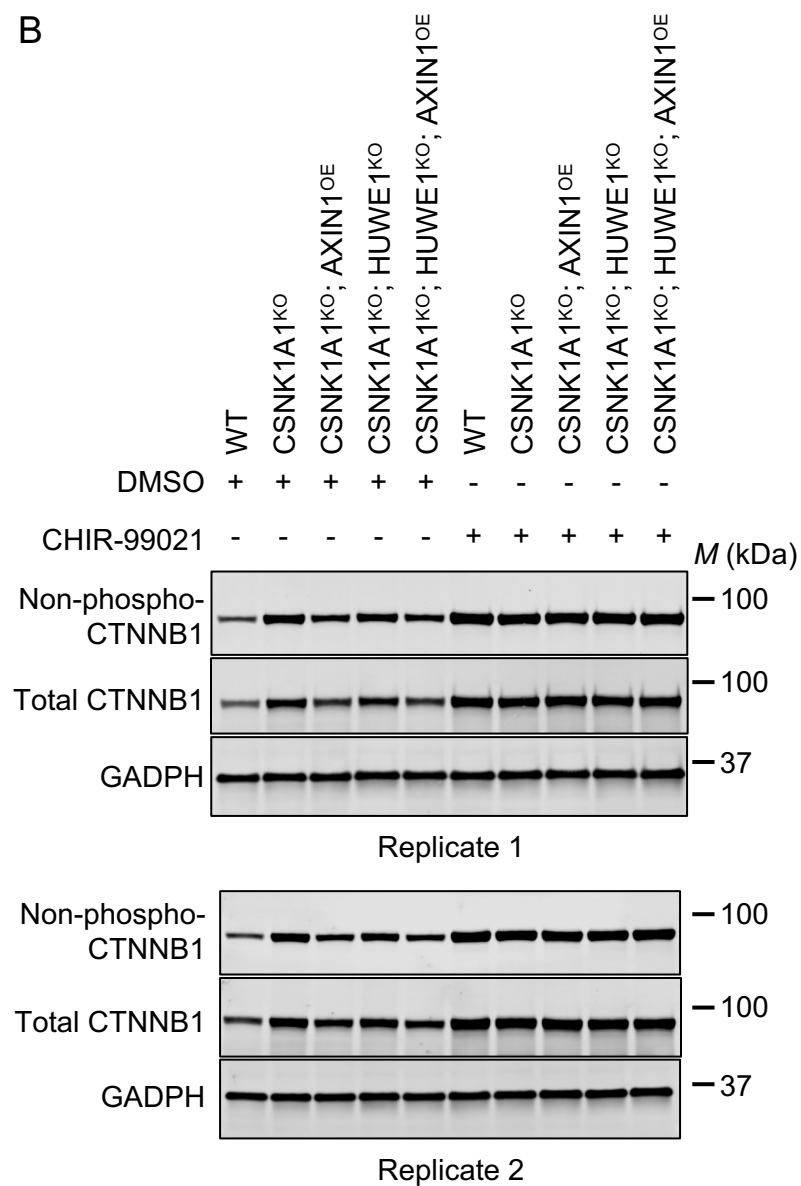
1475

S1 Fig

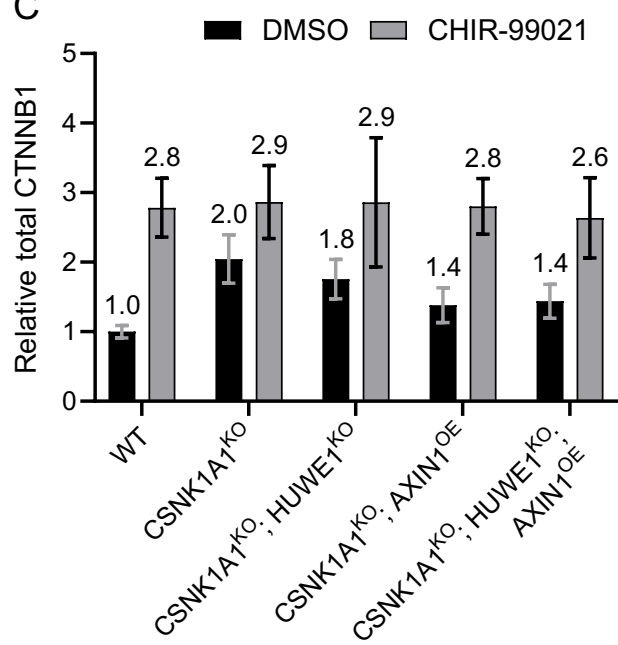
A



B



C



D

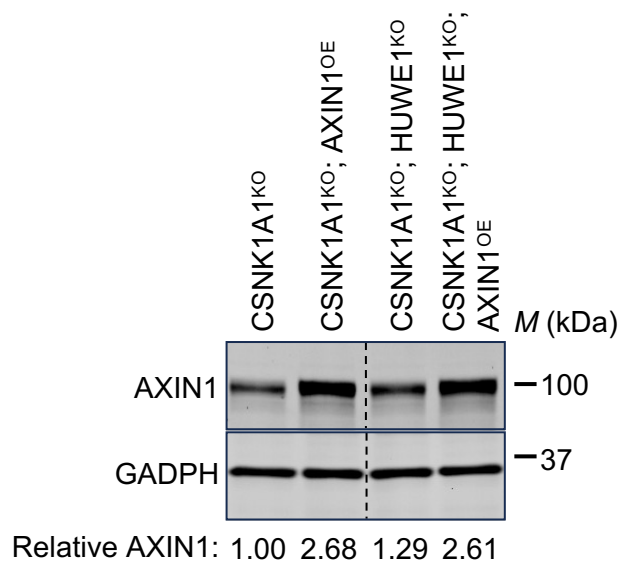
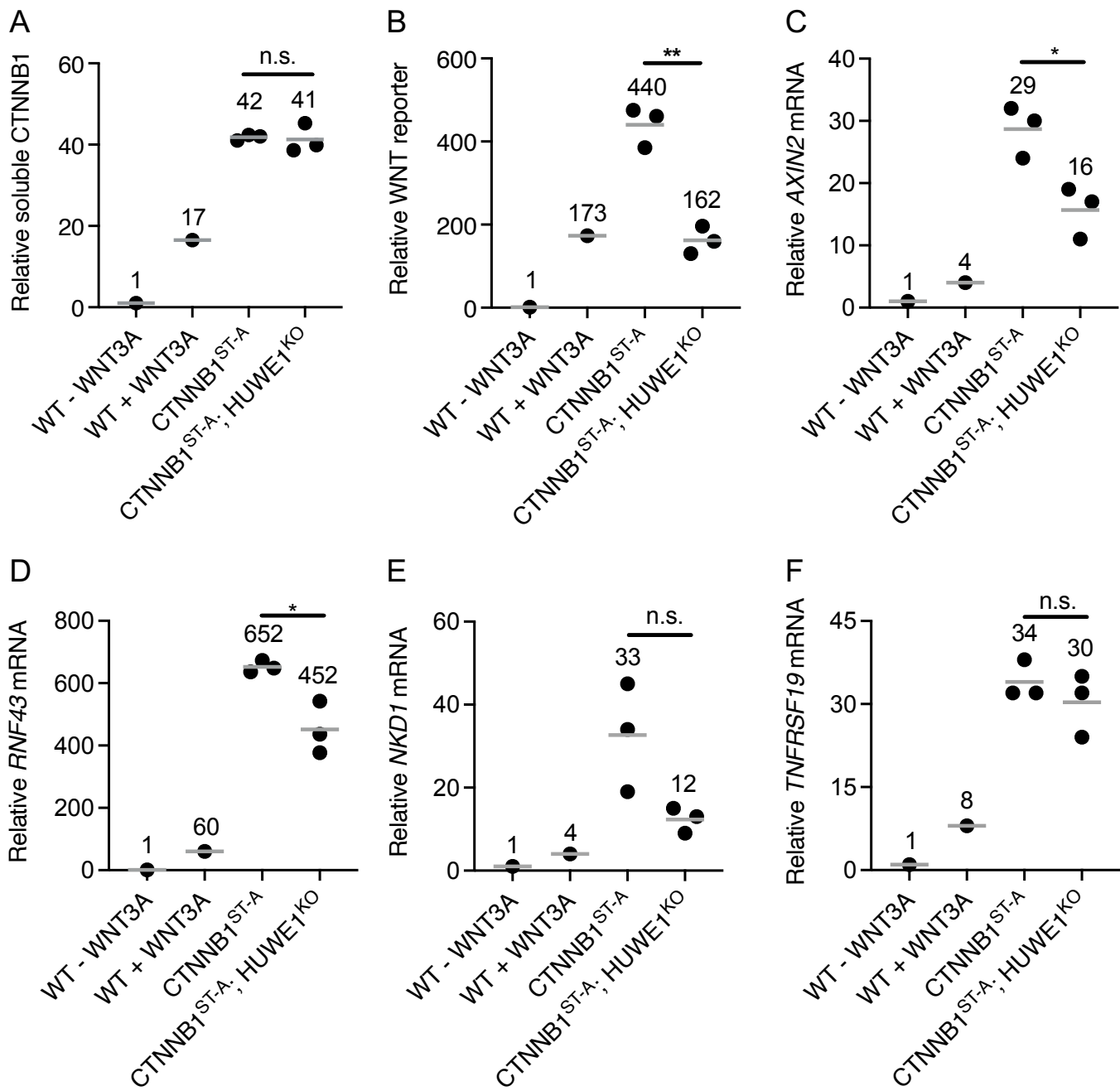


Fig 2



A

CTNNB1 phosphodegron

CTNNB1^{WT}: CTG GAC TCT GGA ATC CAT TCT GGT GCC ACT ACC ACA GCT CCT TCT CTG

CTNNB1^{ST-A}: CTG GAC TCT GGA ATC CAT **GCT** GGT GCC ACT **GCC** ACA GCT CCT **GCT** CTG

CTNNB1^{WT}: L31, D32, S33, G34, I35, H36, S37, G38, A39, T40, T41, T42, A43, F44, S45, L36

CTNNB1^{ST-A}: L31, D32, S33, G34, I35, H36, **A37**, G38, A39, T40, **A41**, T42, A43, F44, **A45**, L36

Kinase:

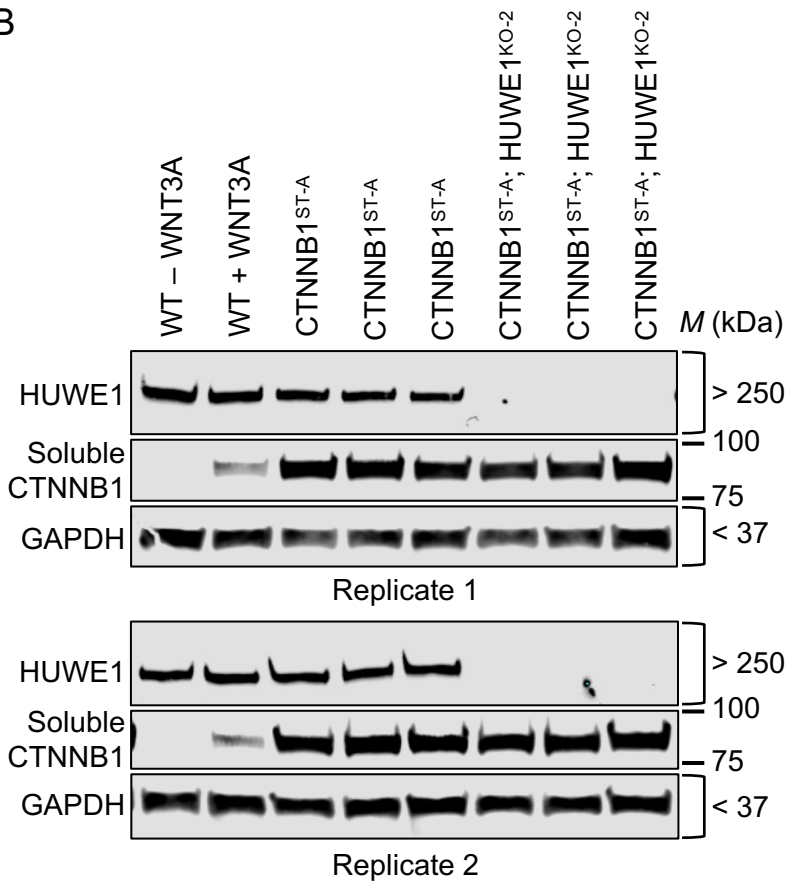
GSK3A/B

GSK3A/B

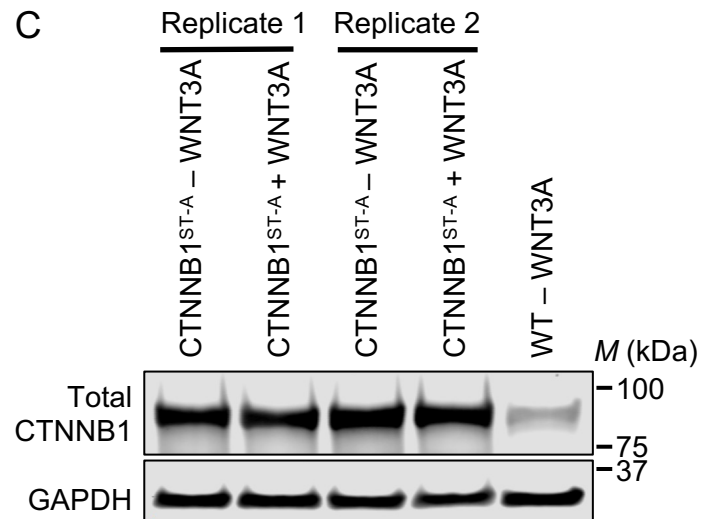
GSK3A/B

CSNK1A1

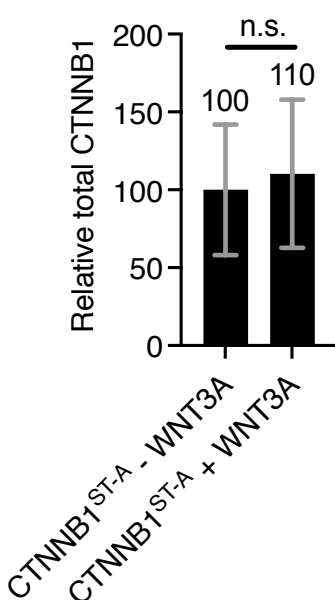
B



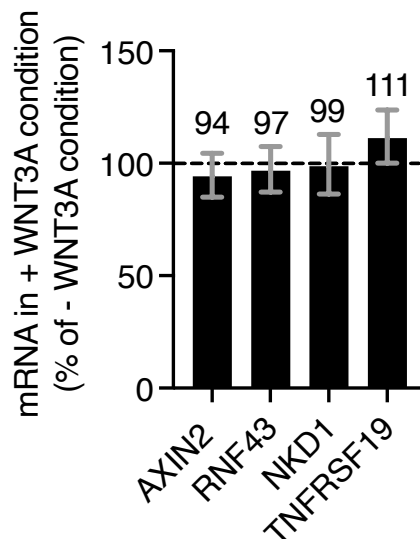
C



D



E



F

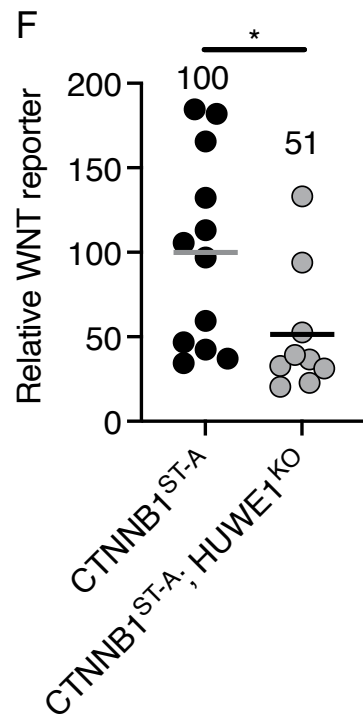
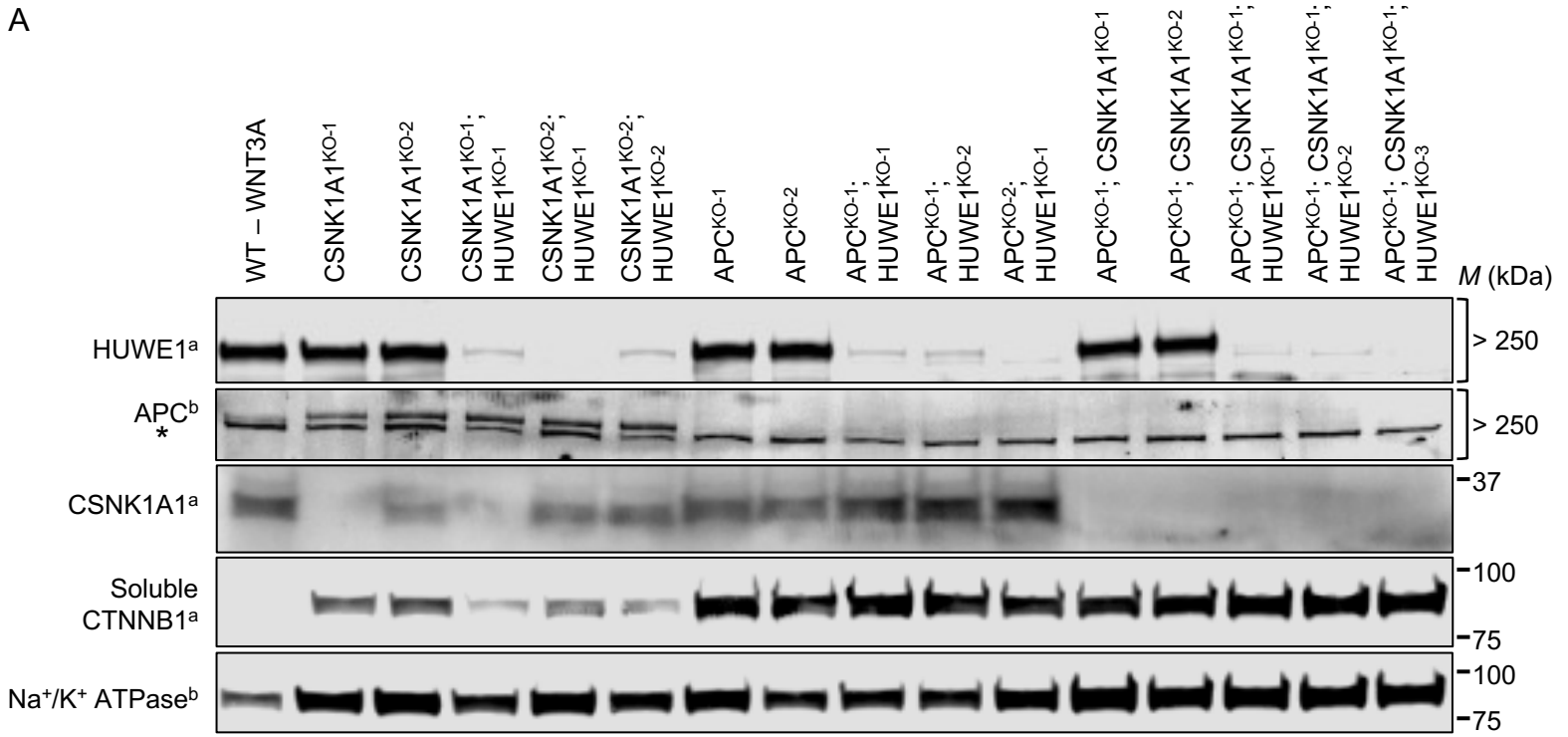
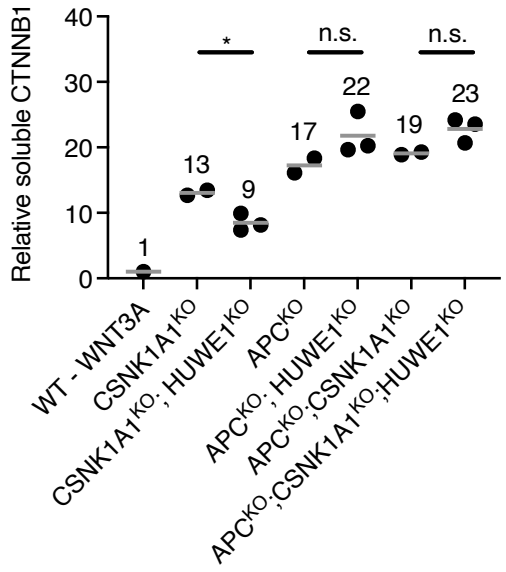


Fig 3

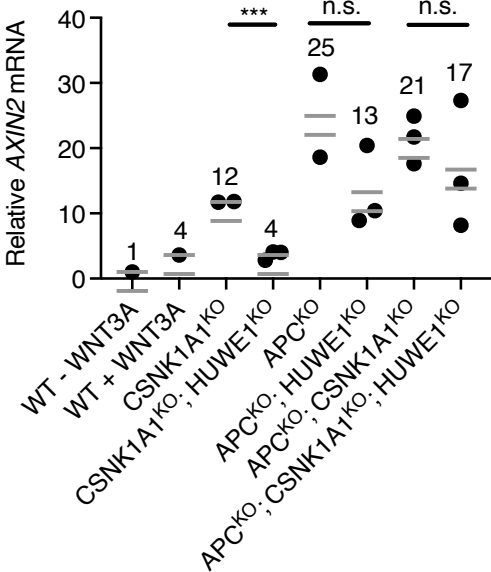
A



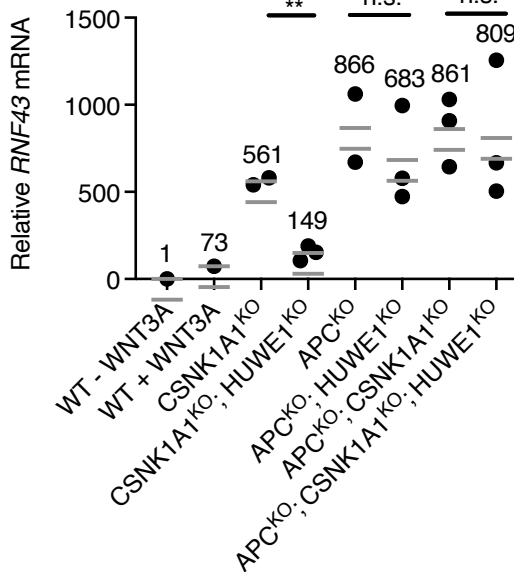
B



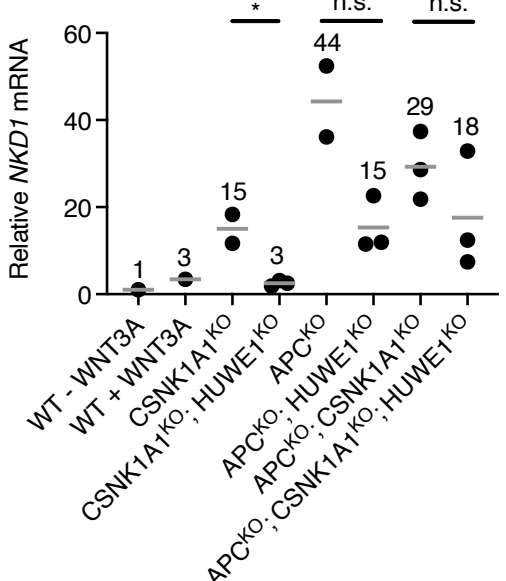
C



D



E



F

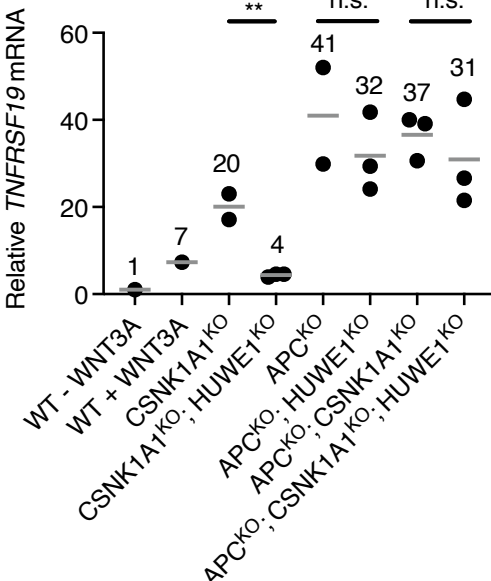
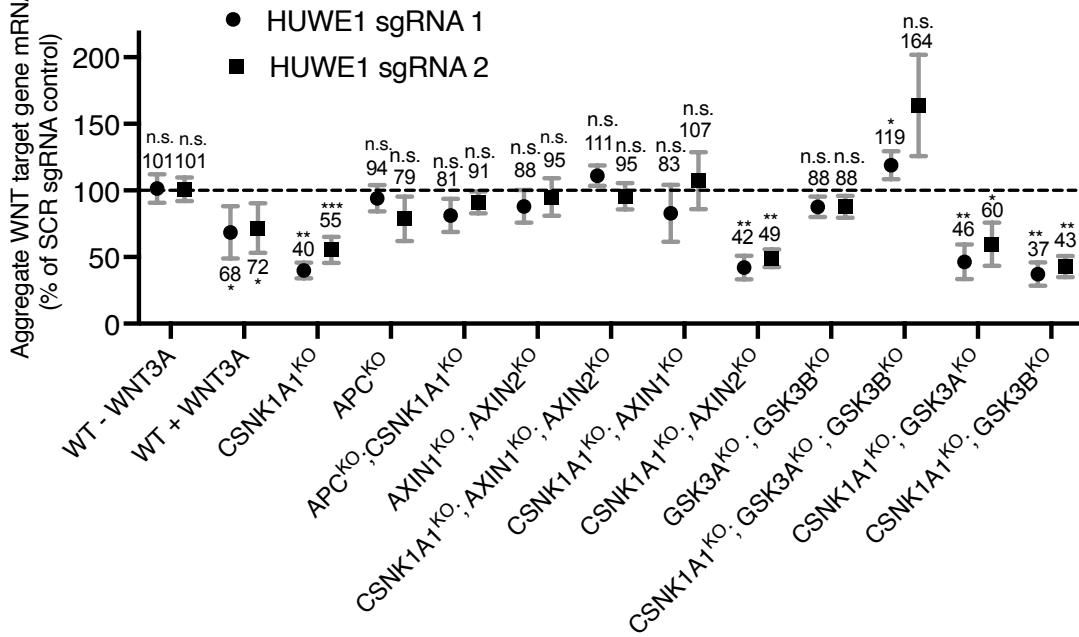
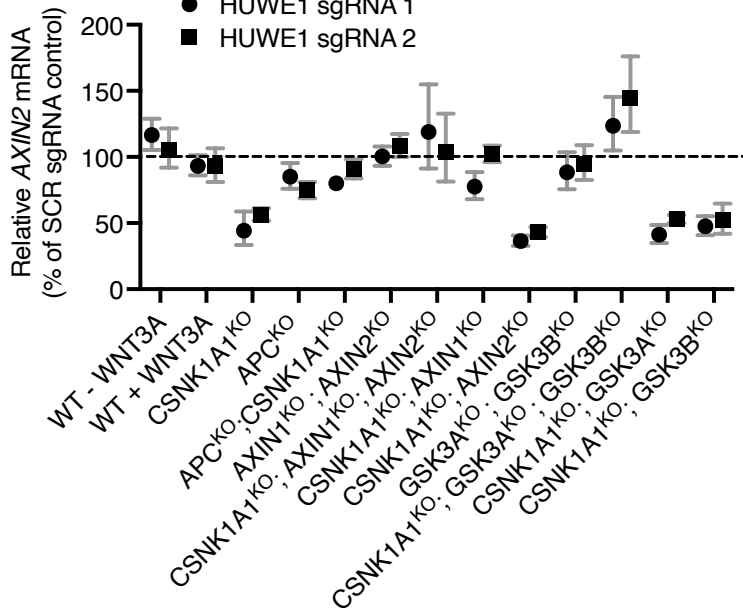


Fig 4

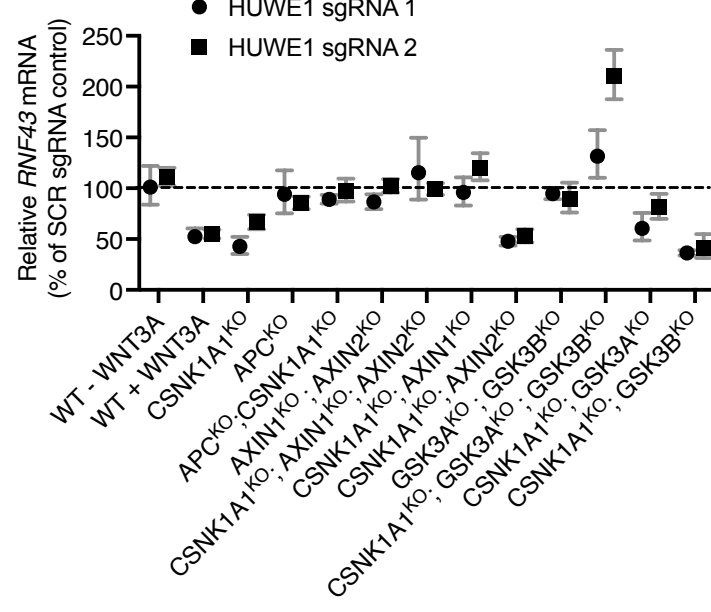
A



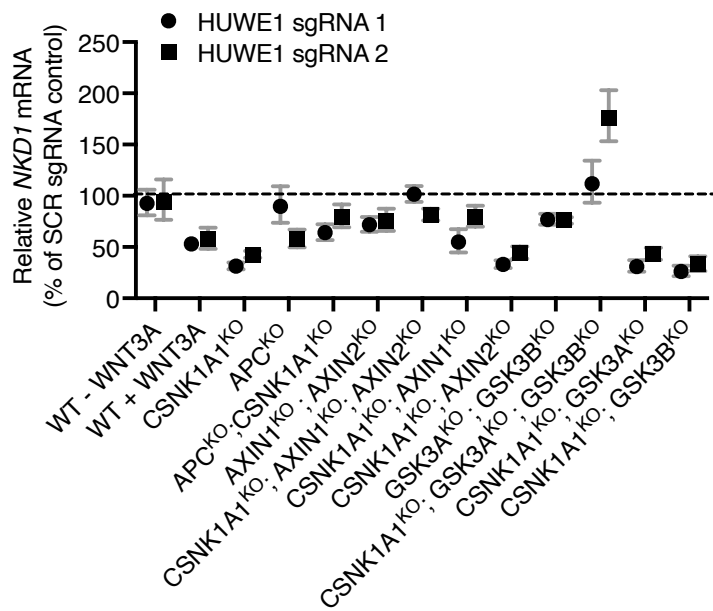
B



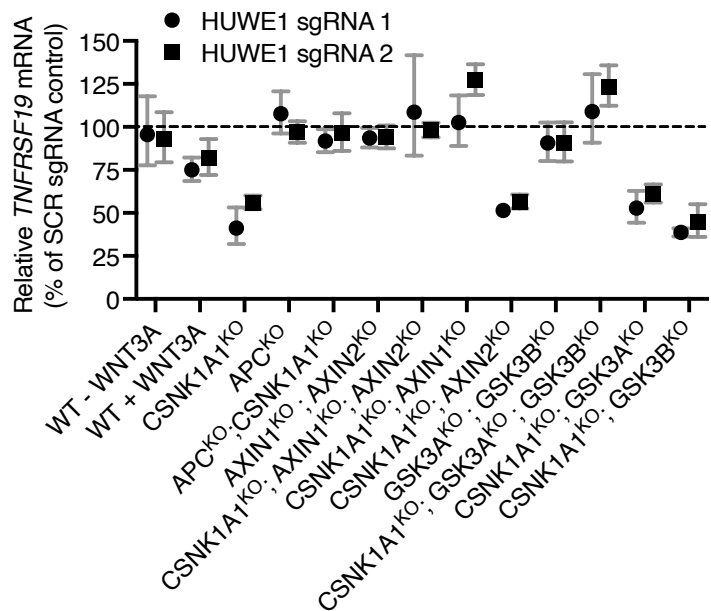
C



D

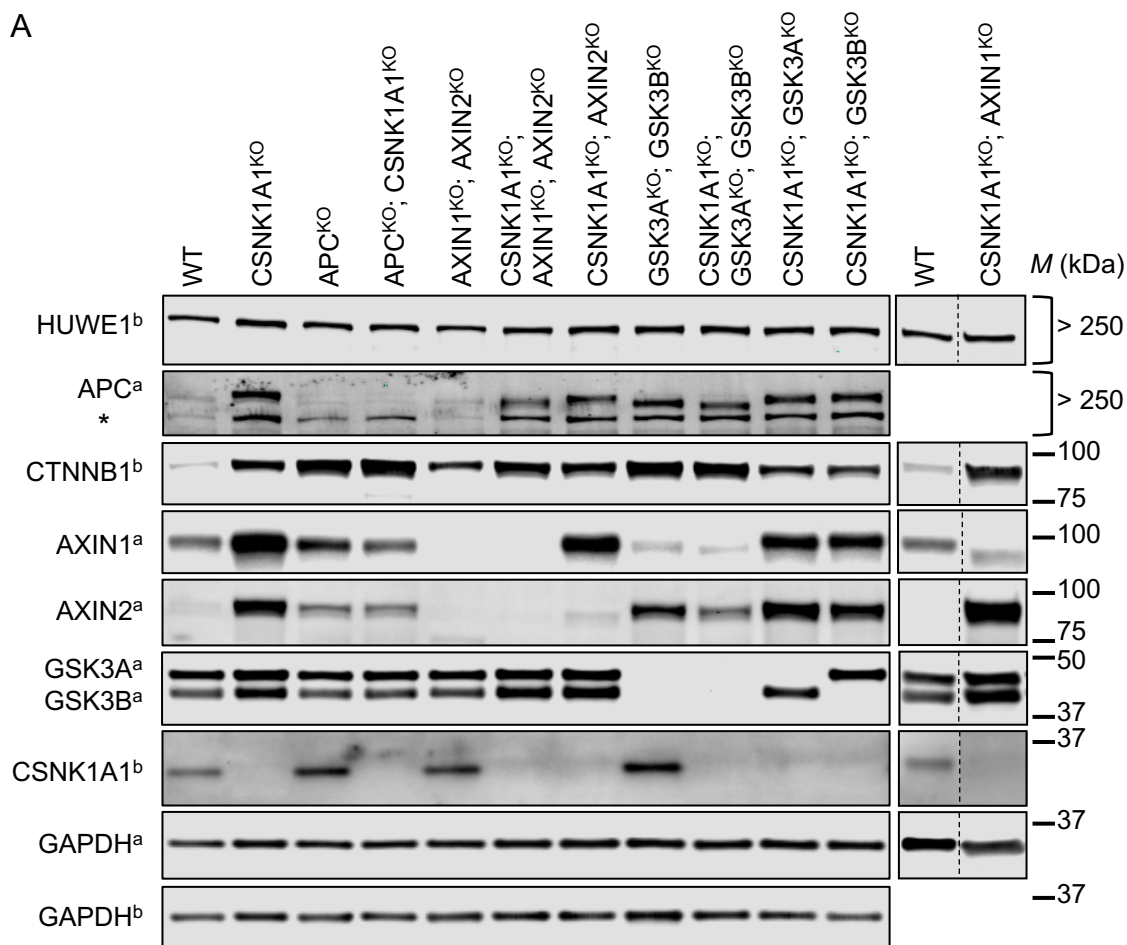


E

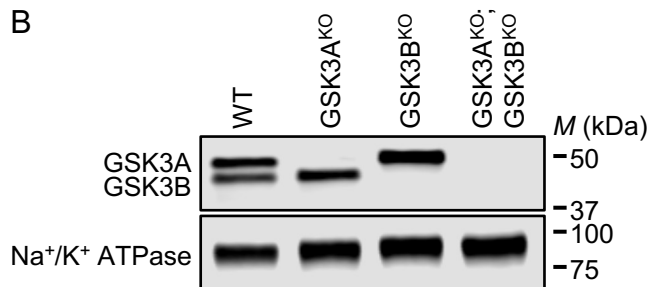


S4 Fig

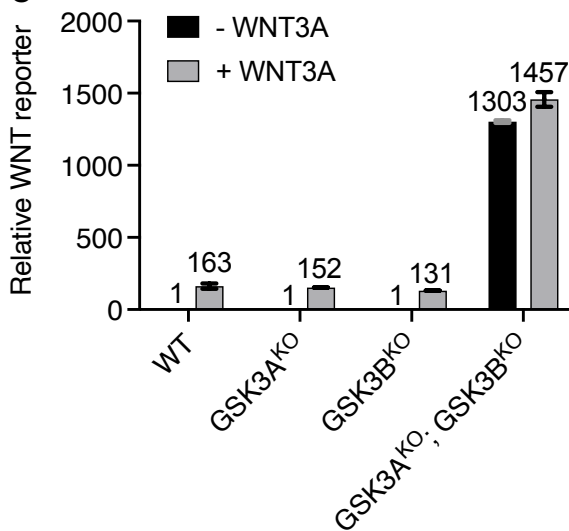
A



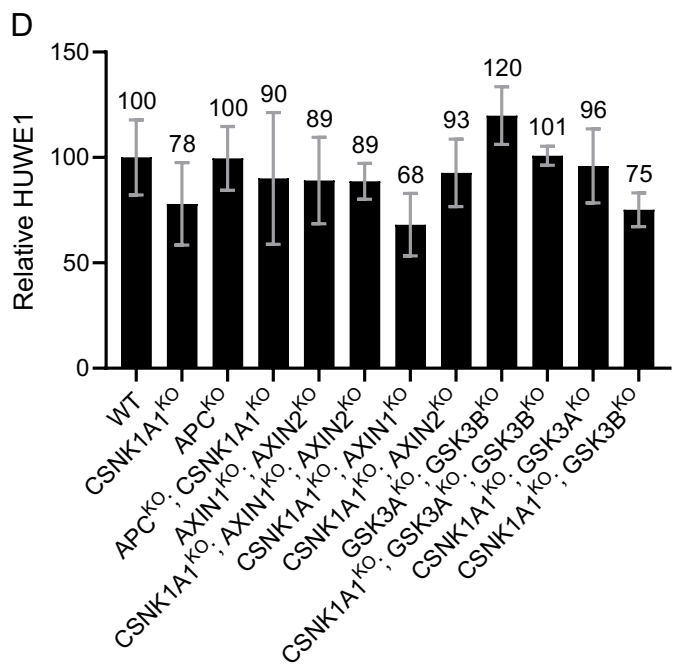
B



C

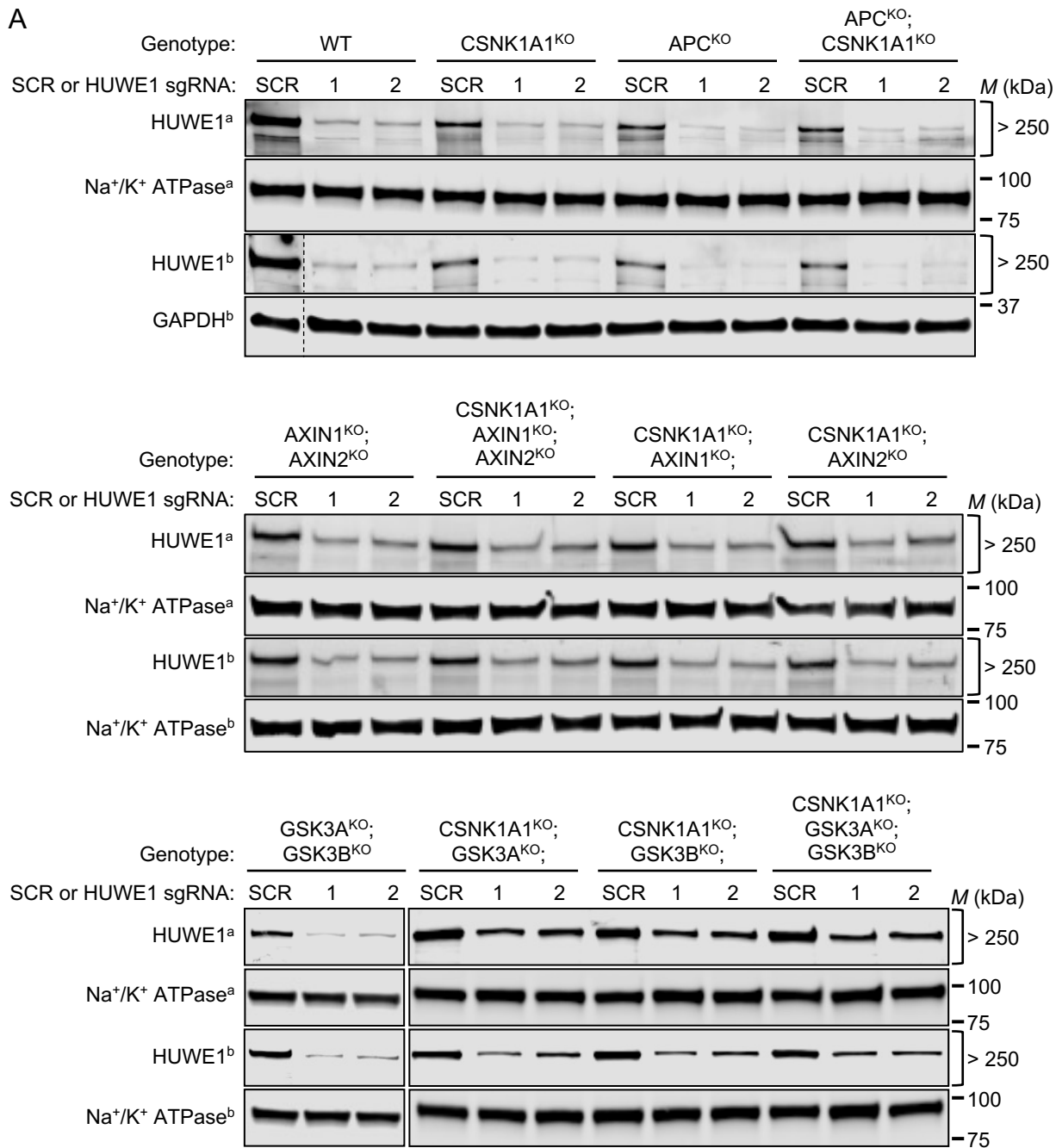


D



S5 Fig

A



B

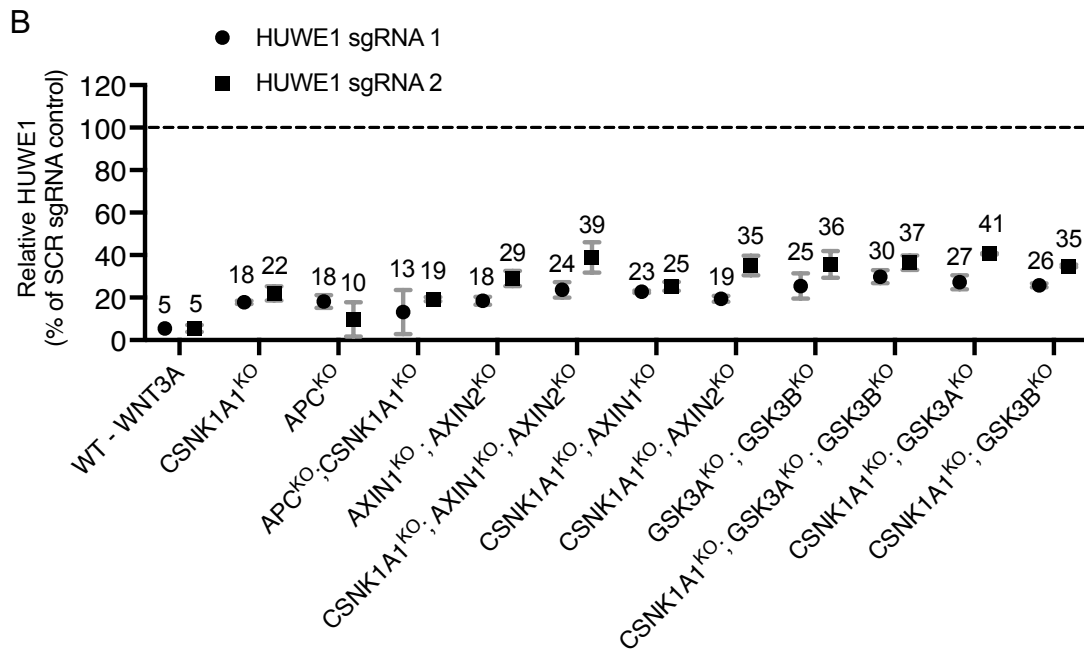
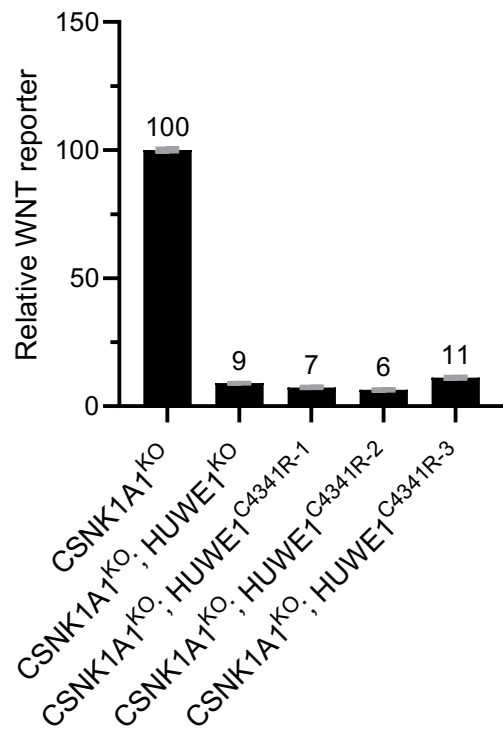
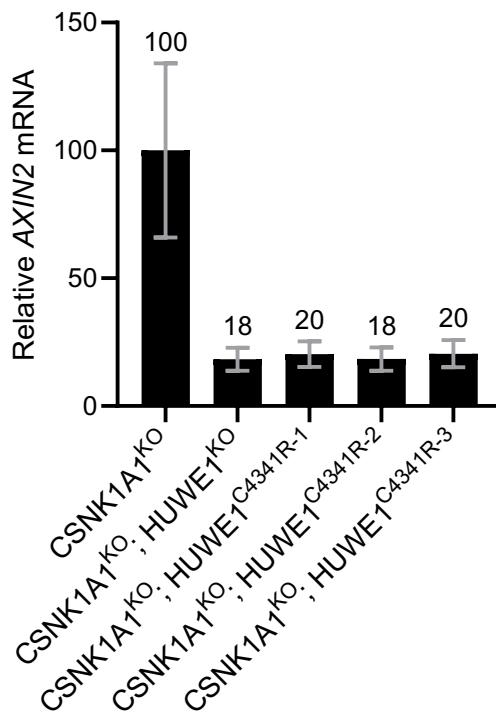


Fig 5

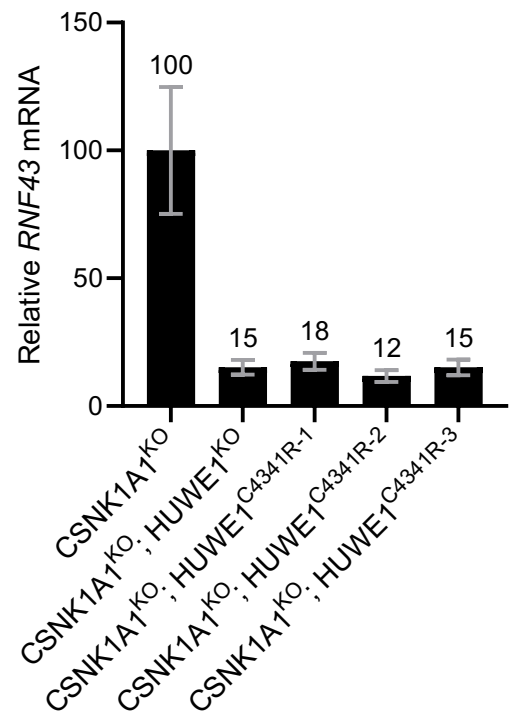
A



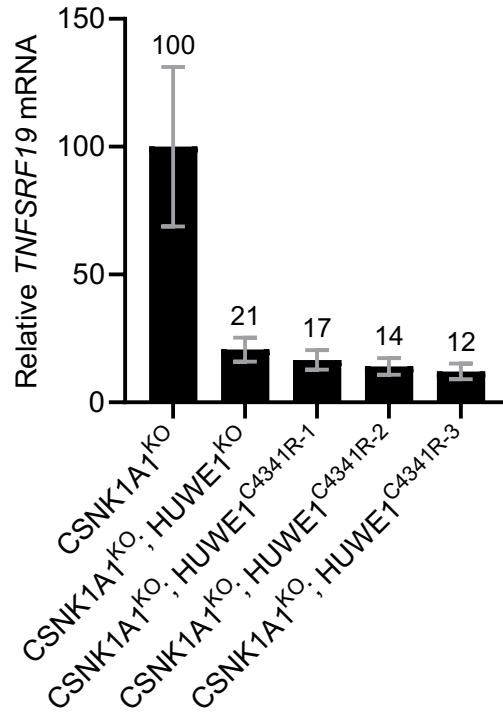
B



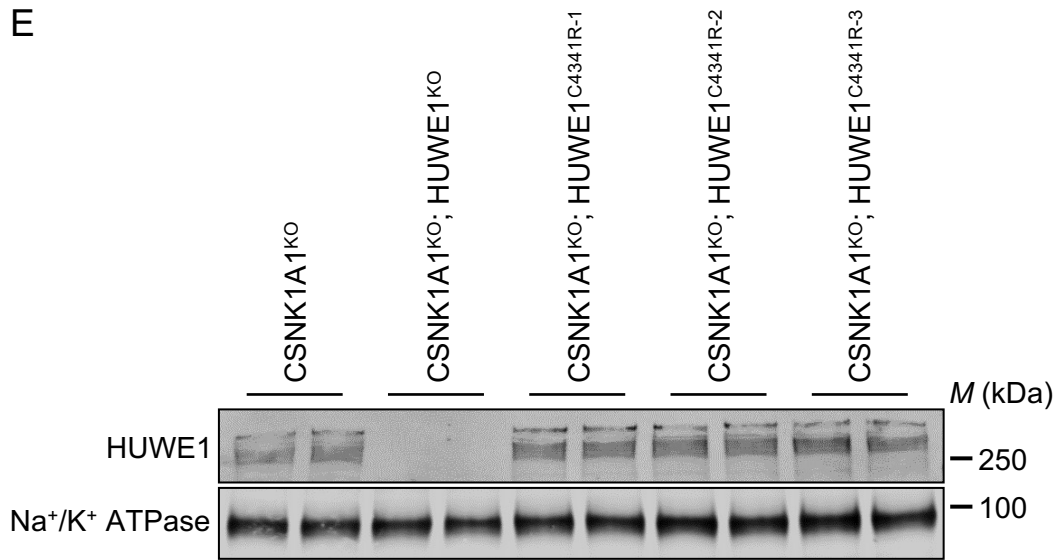
C



D

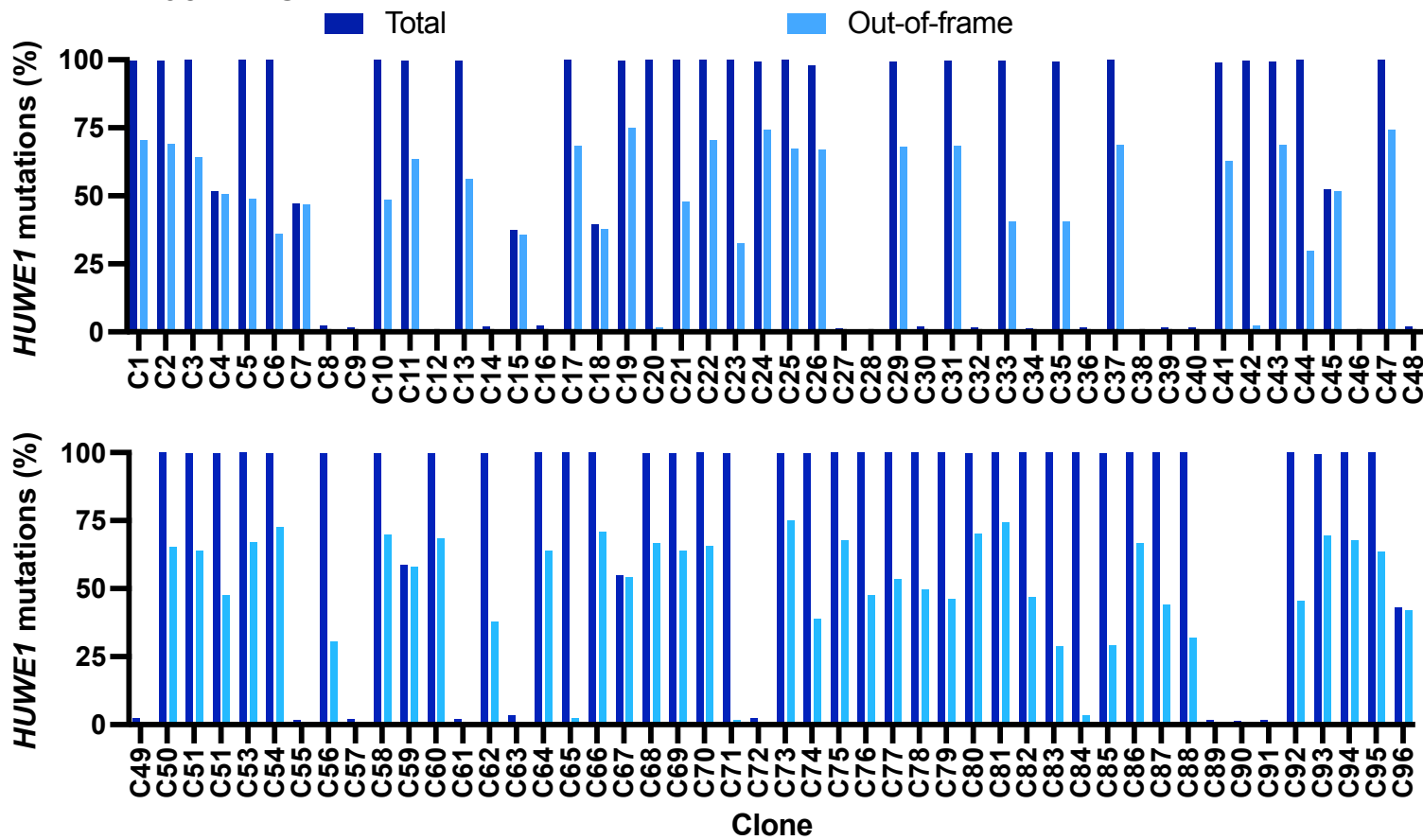


E



S6 Fig

A HEK293T-7TG

B HEK293T-7TG CSNK1A1^{KO}